NAVAL POSTGRADUATE SCHOOL

MONTEREY, CALIFORNIA

THESIS

COMPUTER SIMULATIONS OF CORONARY BLOOD FLOW THROUGH A CONSTRICTION

by

David M. New
Luis E. Estrada

March 2014

Thesis Advisor:	Bruce Denardo
Co-Advisor:	Gamani Karunasiri
Co-Advisor:	Scott Denardo

Approved for public release; distribution is unlimited

THIS PAGE INTENTIONALLY LEFT BLANK

REPORT DOCUMENTATION PAGE

Form Approved OMB No. 0704-0188

1. AGENCY USE ONLY *(Leave blank)*	**2. REPORT DATE** March 2014	**3. REPORT TYPE AND DATES COVERED** Master's Thesis

4. TITLE AND SUBTITLE
COMPUTER SIMULATIONS OF CORONARY BLOOD FLOW THROUGH A CONSTRICTION

5. FUNDING NUMBERS

6. AUTHOR(S) David M. New and Luis E. Estrada

7. PERFORMING ORGANIZATION NAME(S) AND ADDRESS(ES)
Naval Postgraduate School
Monterey, CA 93943-5000

8. PERFORMING ORGANIZATION REPORT NUMBER

9. SPONSORING /MONITORING AGENCY NAME(S) AND ADDRESS(ES)
N/A

10. SPONSORING/MONITORING AGENCY REPORT NUMBER

11. SUPPLEMENTARY NOTES The views expressed in this thesis are those of the author and do not reflect the official policy or position of the Department of Defense or the U.S. Government. IRB Protocol number ____N/A____.

12a. DISTRIBUTION / AVAILABILITY STATEMENT
Approved for public release; distribution is unlimited

12b. DISTRIBUTION CODE
A

13. ABSTRACT (maximum 200 words)

Stenoses (blockages) in coronary arteries cause heart attack, which the Centers for Disease Control and Prevention ranks as the leading cause of death among American adults. We have performed computer simulations in order to understand the flow patterns due to stenoses with and without a guidewire used for interventional procedures (e.g., stent deployment). Building off previous models that have been partially validated with experimental data, this thesis continues to develop the models in order to further evaluate fluid characteristics for cardiovascular applications. Reasonable agreement occurs between computational and experimental data. This work is done in preparation for future research to develop a microelectromechanical system capable of monitoring blood flow and aiding in medical diagnoses.

14. SUBJECT TERMS COMSOL, Stenosis, Fluid Dynamics, Hemodynamics, Slip

15. NUMBER OF PAGES
63

16. PRICE CODE

17. SECURITY CLASSIFICATION OF REPORT	**18. SECURITY CLASSIFICATION OF THIS PAGE**	**19. SECURITY CLASSIFICATION OF ABSTRACT**	**20. LIMITATION OF ABSTRACT**
Unclassified	Unclassified	Unclassified	UU

NSN 7540-01-280-5500 Standard Form 298 (Rev. 2-89)
Prescribed by ANSI Std. 239-18

THIS PAGE INTENTIONALLY LEFT BLANK

Approved for public release; distribution is unlimited

COMPUTER SIMULATIONS OF CORONARY BLOOD FLOW THROUGH A CONSTRICTION

David M. New
Lieutenant, United States Navy
B.S., United States Naval Academy, 2006

Luis E. Estrada
Lieutenant, United States Navy
B.S., University of Texas, 2007

Submitted in partial fulfillment of the
requirements for the degree of

MASTER OF SCIENCE IN ENGINEERING ACOUSTICS

from the

NAVAL POSTGRADUATE SCHOOL
March 2014

Authors: David M. New
Luis E. Estrada

Approved by: Bruce Denardo
Thesis Advisor

Gamani Karunasiri
Co-Advisor

Scott Denardo
Co-Advisor

Daphne Kapolka
Chair, Engineering Acoustics Academic Committee

THIS PAGE INTENTIONALLY LEFT BLANK

ABSTRACT

Stenoses (blockages) in coronary arteries cause heart attack, which the Centers for Disease Control and Prevention ranks as the leading cause of death among American adults. We have performed computer simulations in order to understand the flow patterns due to stenoses with and without a guidewire used for interventional procedures (e.g., stent deployment). Building off previous models that have been partially validated with experimental data, this thesis continues to develop the models in order to further evaluate fluid characteristics for cardiovascular applications. Reasonable agreement occurs between computational and experimental data. This work is done in preparation for future research to develop a microelectromechanical system capable of monitoring blood flow and aiding in medical diagnoses.

THIS PAGE INTENTIONALLY LEFT BLANK

TABLE OF CONTENTS

THIS PAGE INTENTIONALLY LEFT BLANK

LIST OF FIGURES

ACKNOWLEDGMENTS

We would like to thank our advisors for their continuous assistance and unfaltering support in the completion of this thesis.

- Dr. Bruce Denardo, for his expertise and ensuring our research stayed true to course.
- Dr. Gamani Karunasiri, for his ability to come up with solutions when it looked like our research would come to a halt.
- Dr. Scott Denardo, for providing the experimental data and insights into application of the experimental data and computer simulations into the clinical setting.
- Lieutenant Tom Dean, for spearheading this research topic and being able to follow in his footsteps.

We would also like to thank John Dunec of COMSOL multiphysics, whose help and thorough knowledge of the software enabled us to accomplish this work.

THIS PAGE INTENTIONALLY LEFT BLANK

I. INTRODUCTION

A. BACKGROUND

The leading cause of death in United States adults is heart attack, according to the Centers for Disease Control and Prevention. This is generally caused by a constriction of a coronary artery through a process known as atherosclerosis, or an increased amount of plaque building on the walls of the artery eventually restricting flow. This can be particularly dangerous due to the risk of a blood clot (known as thrombus) forming on the surface of the plaque or a piece of the plaque breaking off. Either of these situations could result in a complete blockage of an artery resulting in life threating medical conditions (e.g., heart attack).

The most common invasive treatment for a blocked artery is the use of a technique known as *angioplasty*. In this procedure, a balloon is carefully placed within the artery and inflated in order to re-widen the artery and increase blood flow. Generally a stent, or a mesh wire tube, is permanently inserted in order to scaffold open the artery wall following the angioplasty (Denardo et al., 1994).

Unfortunately, stents have a non-trivial rate of failure. Depending on patient characteristics (e.g., diabetes), artery characteristics (e.g., diameter) and design of the stent (e.g., bare metal vs. drug eluting), the risk of the stenosis (blockage) returning and causing failure can be as high as 30% within the first year for a diabetic patient with a small diameter artery undergoing bare metal stent deployment (Leimgruber et al., 1986). However, there is currently no method for definitively determining if restenosis has occurred without an invasive procedure to determine the status of the artery in question. While these procedures have become low risk and routine, they remain fairly expensive and, as with all procedures, they carry some small but real risk of complication.

One possible solution for this issue is to attach a MEMS device to the stent placed into the artery. This device would contain a sensor capable of taking real time measurements of either blood flow or pressure and transmitting this data remotely to be analyzed. By monitoring an individual's blood flow through the artery, doctors would be

able to notice a change in blood flow indicative of a stenosis prior to any harmful effects taking place and without any of the risk which comes from an additional procedure.

Creating an appropriate device would require four parts: a sensor, a power source, a transmitter, and a receiver. Each of these components requires specific characteristics to operate within the artery that will be challenging to overcome. The first of these challenges is determining a sensor capable of accurately measuring blood flow. The sensor will face severe size limitations due to the relatively small diameter of coronary arteries (≤4.0 mm). Not only will it need to be small enough to fit on the stent, but it also must not interfere with blood flow enough to function as a blockage of its own or pose any risk of aggravating pre-existing coronary conditions.

Adding a traditional battery-powered source will require more space to be utilized by the device and would have to also be attached to the stent, further increasing the risk of the device interfering with blood flow. A more ideal solution would be to have the device powered by the flow itself (as with using piezoelectric material).

As with the other components, the transmitter will need to be attached to the stent itself in such a manner that it doesn't affect blood flow or increase risk for clot formation. If the device were to transmit constantly, it would not only require more power, but would also require a transmitter strong enough to be capable of transmitting through human flesh, which creates further issues. Another possibility would be a passive system that is queried by an outside source, potentially eliminating the need for an active transmission from the MEMS device.

A passive system would also eliminate certain issues with the receiver. With an active transmitter in the artery, the receiver would need to be sensitive enough to pick up the signal of the transmitter, which would be weak at best. With a query-type system, the majority of the power requirements fall to the receiver. This will send a signal to the actual device. The receiver as the only external component will face no power restrictions, so placing the majority of the power requirements on this component can ease the design requirements.

Due to the complex nature of MEMS devices and the stringent requirements placed on the device by the coronary circulation, the problem is an ideal candidate for computer simulations. Simulations allow for increased flexibility, enabling the analysis of possible components in various locations in order to narrow down possibilities, thus sparing much of the time and expense that goes along with developing and carrying out experiments.

For this thesis, COMSOL multiphysics software (COMSOL Inc., 1998) was selected to create the models needed. COMSOL was selected for its ability to reproduce a variety of physics phenomena, providing flexibility in simulations and allowing the system and device to be modeled and evaluated. Previous COMSOL simulations of flow through stenoses were performed by Dean (2013).

Due to the uncertainty of simulations, models will be compared to known experimental data in order to validate both the software and specific models. Once the models have been confirmed as accurate, they will be used to explore different options to evaluate how both the system and MEMS device react and to determine the best course of action. Then the modified system will be created for experimentation in order to prove the functionality of the device as well as reconfirm the accuracy of the model.

B. PRIOR WORK

1. Experimental Data

The initial experimental data were collected by Denardo et al. (1994) using a scaled-up model of coronary blood flow (Figure 1) and a Laser Doppler Velocimeter (LDV). The portion of the model that was being tested was made from acrylic tube with an internal diameter of 2.54 cm. Clear acrylic was selected due to the limitation of the LDV that requires optical clarity.

In order to ensure laminar flow for the entrance to the testing region, the test section length was 233 cm. A constant pressure head reservoir with an overflow pipe maintained stable pressure and continuous flow. A gate valve was adjusted to obtain the desired Reynolds number. Reynolds number was calculated as

$$Re = \frac{\rho v D}{\mu} \quad (1)$$

where Re is the unitless Reynolds number, ρ is the fluid density in kg/m^3, μ is the dynamic viscosity in Pa*s, v is the average flow velocity and D is the inside diameter in meters.

The system used roughly a 50% mixture of glycerol and water at various speeds in order to maintain constant Reynolds numbers (Re) at 200, 300 and 400. Due to the changing nature of the mixture in use, characteristics of the fluid were determined through the use of standard tables prior to gathering each set of LDV data.

Acrylic axisymmetric stenoses, modeled in Figure 2, were inserted to create constrictions of 20, 40, 60, 75 and 90% by cross sectional area. These stenoses began at the outside wall of the tube and angled inward, each with 45 degree edges relative to the direction of the tube wall, necessitated in order to gain accurate readings from the LDV. Each stenosis was two cylinder diameters in length at their exterior, regardless of their width.

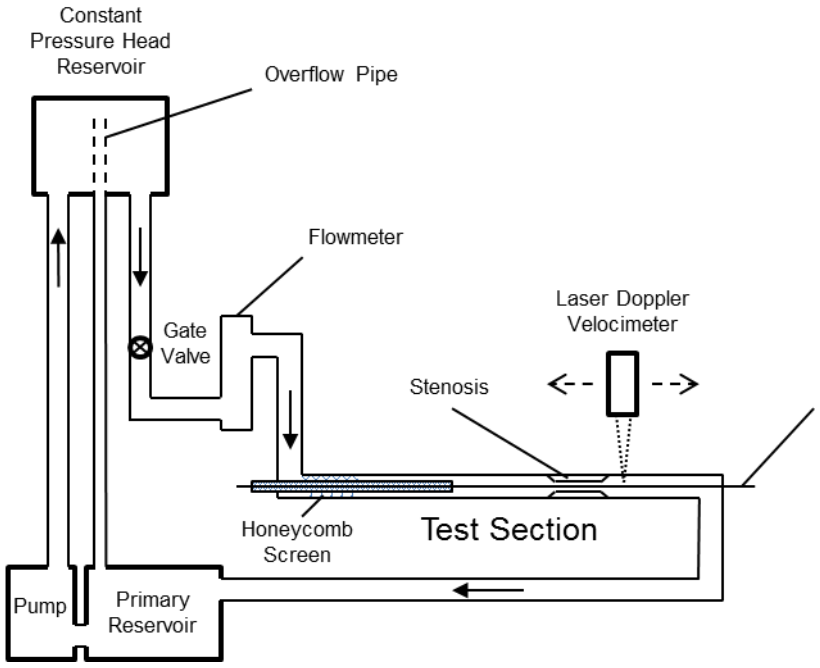

Figure 1. Scaled model of artery with stenosis used for experimental data (after Denardo, 1994).

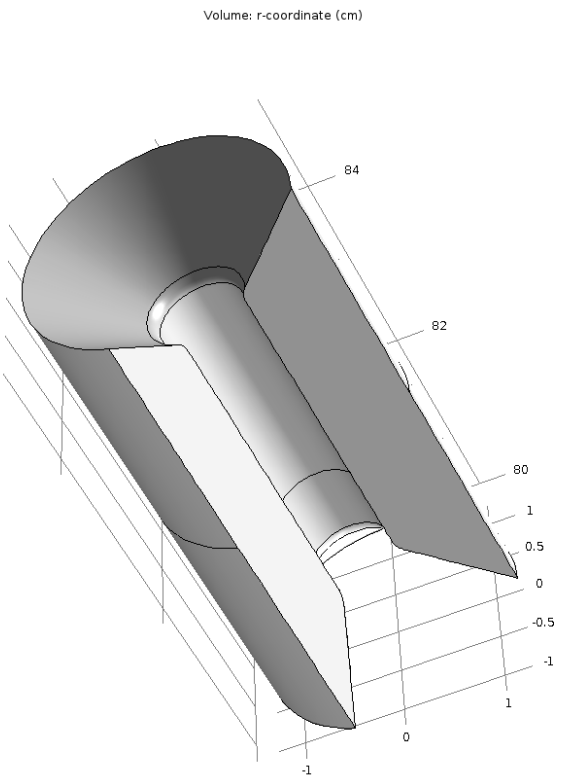

Figure 2. Schematic representation of the shape of the 90% stenosis with a cutaway. All units are in centimeters.

Velocity measurements were taken at nine axial locations. For this thesis, negative numbers will denote upstream locations, and the axial measurements are given in terms of multiples of the tube diameter relative to the center of the stenosis. Measurements were taken upstream at locations -1.500D, -1.000D, and -0.475D, at the center of the stenosis (0.000D) and downstream at +0.475D, +1.000D, +2.000D, and +2.500D. At each of these positions, measurements were taken at 1 mm radial increments. The measurements at the +/-0.475D marks were in order to capture the flow at the edges of the stenoses. Focus was placed on downstream flow instead of upstream due to the desire to capture the effects of the blockage downstream. Cengel and Cimbala (2006) provide a formula for the axial velocity profile u(r) for flow in a pipe given by

$$u(r) = 2 \times u_{avg}\left(1 - \frac{r^2}{R^2}\right) \quad (2)$$

where u_{avg} is the average fluid velocity in m/s, R is the radius of the cylinder (1.27 cm for the experiment) and u(r) is the velocity as a function of the radius from the center of the tubing, r. The quantity u_{avg} is equal to half the maximum velocity for fully laminar flow. This equation is a solution to the Hagen-Poiseuille equation that assumes no-slip boundary condition at the pipe wall and fully developed laminar flow.

All of the data points were taken twice for each stenosis, once without and then once with a scaled up guidewire. The guidewire in use was a 0.5 cm diameter stainless steel rod inserted into the center of the tubing. This rod was painted flat black so as to not interfere with LDV readings.

The LDV used to collect the data was a Lexus Model 85 (Palo Alto, CA) with a single color argon laser using a wavelength of 514.5 nm. A system of mirrors was used to reflect the beam into the laser splitter (TSI Model 915 transmitter optics, TSI Model 918 receiving optics). The photomultiplier tube (RCA Model 4526, Somerville, NJ; DC power supply Hewlett Packard Model 51 15A, Palo Alto, CA) had a pinhole diameter of 0.203 m. A TSI Model 550 Intelligent Flow Analyzer was used as the signal processor to analyze the data in real time. Net radial position error of the system was within $\pm$ 0.150 mm, with the optics placed 19.0 cm from the sample (Denardo 1994).

2. Modeling

Building off the work of Denardo (1994), Dean (2013) modeled these systems using COMSOL multiphysics software. Using computer models, he was able to mimic each of the 10 possible configurations and compare the results to the experimental 200 Reynolds number experimental data to judge the accuracy of the simulations.

Due to the axisymmetric nature of the system, a 2D model was used, creating only the aspect of the system that was of interest. As a result, the model consisted of only a set of tubing with the required stenosis, an inlet, an outlet, and the guidewire (as necessary). A catheter was also placed within the model for studies unrelated to his thesis. (Dean, 2013) For this reason, the catheter (shown in Figure 3) was removed in all simulations in this thesis. In order to ensure parabolic laminar flow occurred before

reaching the stenosis, the required entry length was calculated using the equation given by Cengel and Cimbala (2006)

$$Le = 0.05\, Re \times D \tag{3}$$

where Le is the length required in meters, D is the diameter of the tube in meters, and Re is the Reynolds number. For the highest Reynolds number of 400, this resulted in a requirement of 61 centimeters of tubing upstream of the stenosis. A length of 80 centimeters was used upstream instead in order to allow for the required length following the interference caused by the catheter (Dean 2013).

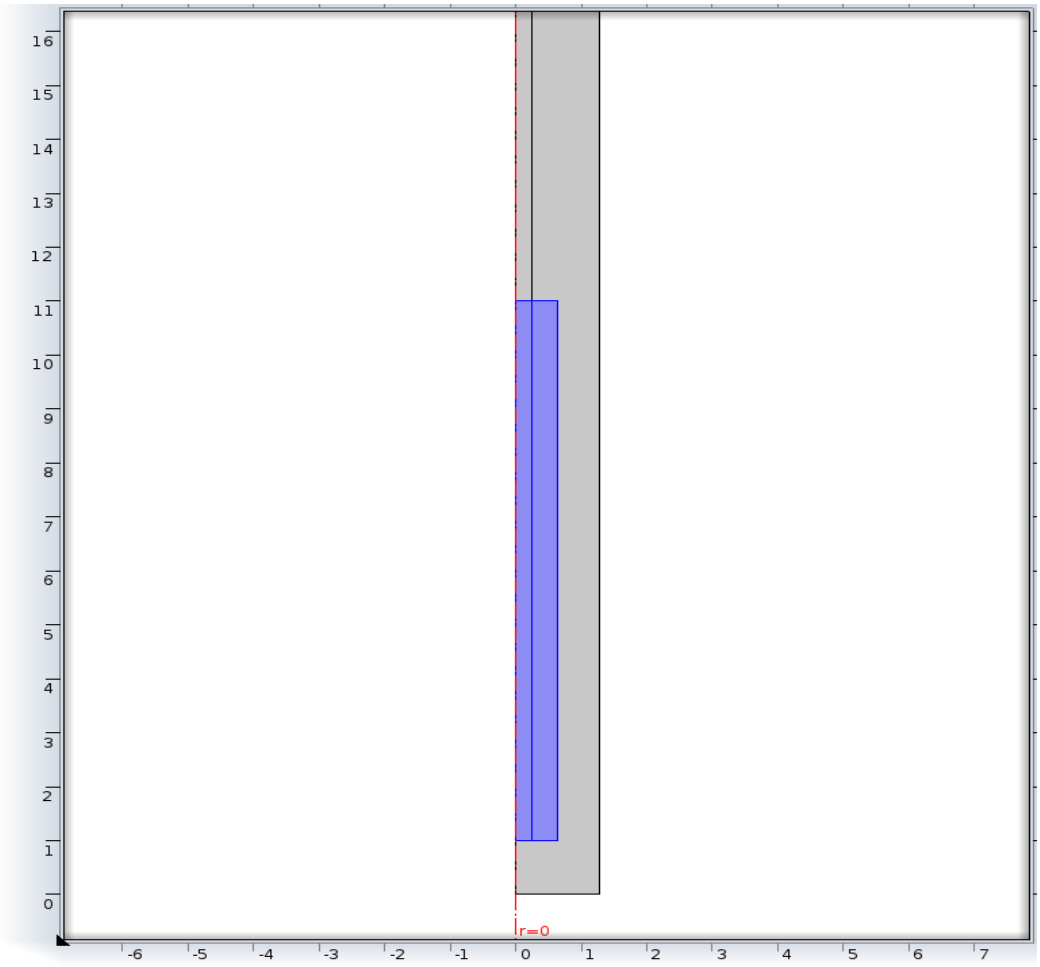

Figure 3. Model inlet with catheter, the catheter is the highlighted section. The stenosis is downstream (not pictured) and the axis of symmetry is located at r=0. All units are in centimeters.

In order to compare the model to the experimental data, the area designated as the test section ranged from -1.5D to +2.5D (Dean 2013) encompassing the area in which measurements were recorded by Denardo (1994). A zoom in of this area is shown in Figure 4. Due to radial symmetry, only half of the tube needs to be included in the model. The stenoses were modeled after those in the in-vitro experiment and share the same dimensions. The guidewire in these models was assumed to be both perfectly straight and perfectly centered in the system with a diameter of 0.508 centimeters (Dean, 2013).

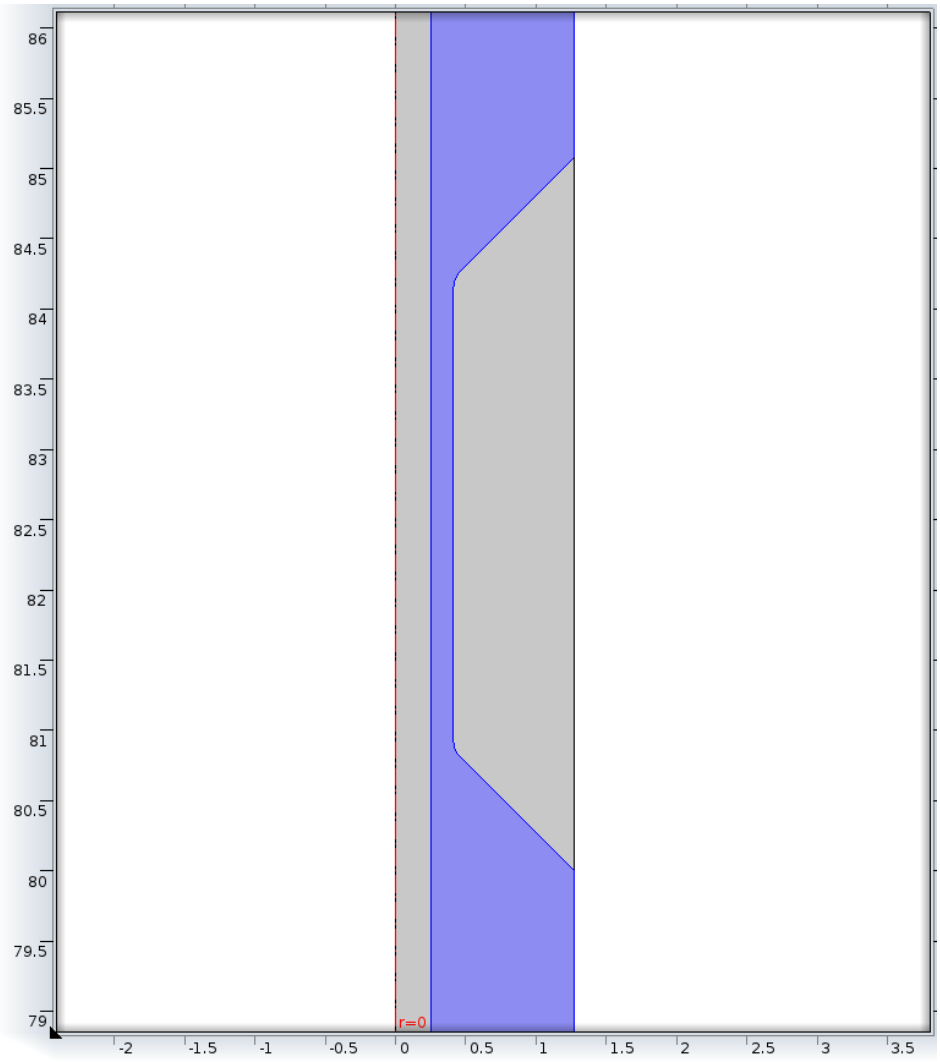

Figure 4. View of the test section of the simulation with a 90% stenosis with guidewire. The axis of symmetry is located at r=0. All units are in centimeters.

Beyond the test section, an additional length of 20 centimeters of tubing was placed in the model to show the downstream effects caused by the stenosis. At the end of this tubing, an outlet boundary condition with pressure set to 0 Pascals gauge pressure and no viscous stress was imposed on the system in order to simulate an indefinite length.

To simulate the fluid used in the experiment, a custom material was created to allow flexibility in matching the characteristics of the mixture used in the experiment. The Laminar Flow module in COMSOL was determined to be adequate to model the flow that occurred in the experiment; however, certain assumptions were required. Most notably the fluid was assumed to be incompressible, and the boundary conditions initially were all assumed to be no-slip with the exception of at the guidewire surface, which was given a moving wall boundary condition. A moving wall boundary condition places a set velocity on the fluid at the point of contact to the boundary. It achieves this velocity at the boundary by simulating that the wall has infinite length and it moves in the direction of fluid flow with a constant velocity that matches the desired boundary condition. During the course of modeling the system, some of the boundary conditions were adjusted, which will be addressed later in this thesis. The inlet velocity for each model was derived from the Reynolds number given in the experiment.

Dean's (2013) simulations at Reynolds number 200 showed remarkably close results to that of the experimental data at lower grade stenoses (20 and 40%). At the higher grade stenoses (60, 75 and 90%), the simulations were still accurate, although differences were more apparent. The rapid rise of velocity at the entrance to the stenosis created some issues for the modeling software, particularly in the cases in which the guidewire was in place. The previous use of a moving wall boundary condition for the guidewire also provided a challenge because it was not physically realizable and proved to be less effective than expected. Thus, a slip velocity boundary condition was used at the guidewire surface instead for all stenoses. The formula used by COMSOL to calculate the value of slip velocity u at a boundary (assuming zero moving wall velocity and no thermal creep effects) is given by:

$$u = L_s * \left| \frac{\partial u}{\partial r} \right| \tag{4}$$

where L_s is the slip length in meters and $|\frac{\partial u}{\partial r}|$ is the magnitude of the derivative of the velocity u in m/s with respect to radial distance r in meters at the boundary. COMSOL calculates this derivative from the tangential shear stress along the boundary and dividing it by the fluid's viscosity (COMSOL, 2013). Figure 5 gives a visual explanation of the slip velocity boundary condition. The wall on the left (r = R) has a no-slip boundary condition and therefore the velocity at the wall goes to zero. The wall on the right ($r = r_0$) has a partial slip boundary condition. By assigning a specific value of slip length Ls and obtaining the value of the slope at the wall from the COMSOL numerical solution a non-zero velocity at the wall is obtained.

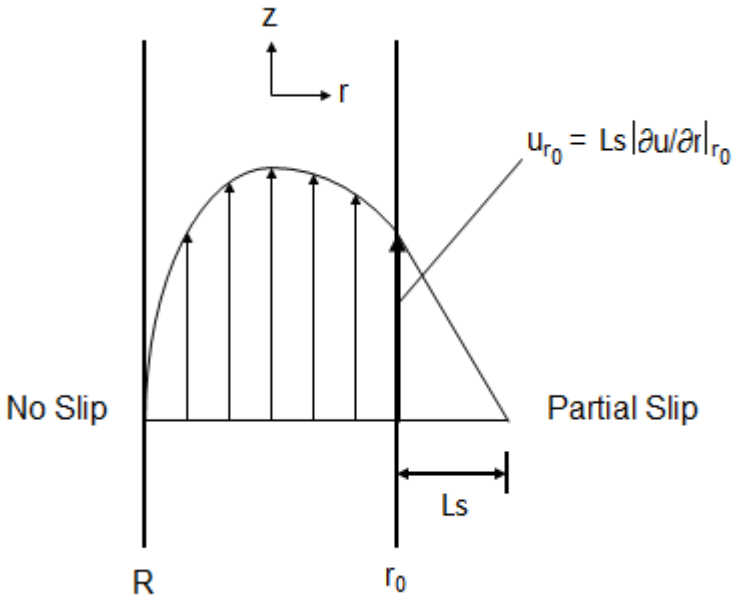

Figure 5. Slip velocity boundary condition.

Dean (2013) showed that experimental data display a linear relationship between Reynolds number and velocity profiles for the case of flow through a stenosis with no guidewire present. Figure 6 re-creates the velocity profile obtained by Dean, along with the velocity profile for the case where the guidewire is present for the 75% stenosis. The linear relationship also holds true for the guidewire case.

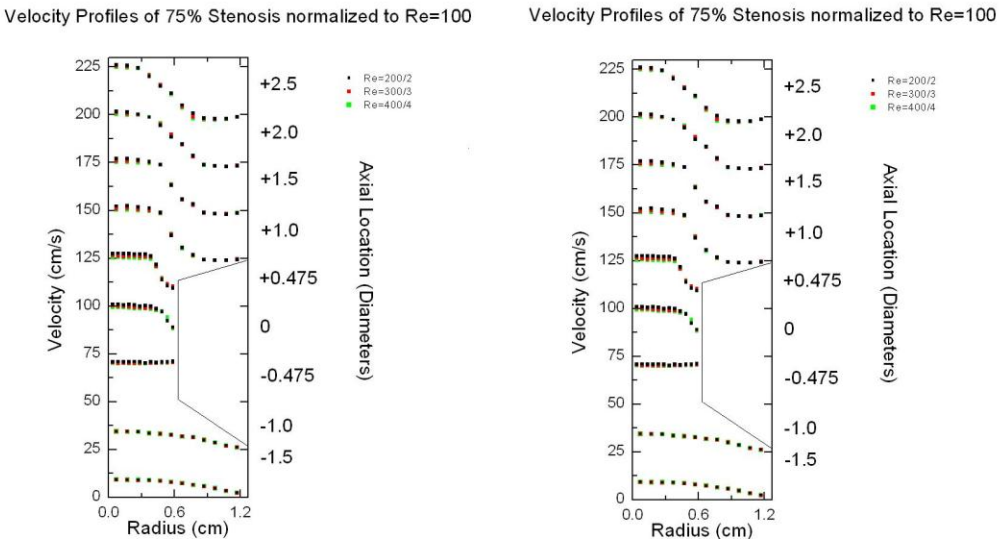

Figure 6. Experimental data for Re 200, 300 and 400 normalized to Re 100. The left profile replicates Dean's work. The right profile shows that the linear relationship in velocity also holds true in the case of the guidewire present.

Dean (2013) was unable to get steady-state results for the 90% stenoses simulations for higher Reynolds numbers. The use of more processing power and the increase in the number of iterations required for the COMSOL solver to achieve a steady state solution enabled the simulations to run for both Reynolds number 300 and 400.

C. APPROACH

This thesis focuses on the next step in developing a model capable of emulating a cardiovascular system by exploring the necessary features of COMSOL. In doing so, we will evaluate the usefulness of COMSOL as a modeling software to understand blood flow in constricted arteries.

This thesis will also address the weaknesses in the previous models in order to continue development toward the end goal of developing a MEMS device capable of monitoring blood flow. Most notably, focus will be placed on the higher-level stenoses in order to address the simulation issues previously recognized. An emphasis will also be

placed on addressing the boundary condition at the guidewire surface in order to ensure accurate modeling in all systems.

II. TIME DEPENDENCY

A. IMPLEMENTATION

Previously completed COMSOL simulations only sought steady state solutions. This was done in order to compare the simulations to the experimental data, which were taken in the steady state condition. In order to continue progress toward accurately modeling a human cardiovascular system and the end goal of developing a MEMs device, a model capable of simulating a time-dependent solution is necessary.

Our initial attempt at time dependency involved changing none of the previously set variables or COMSOL features other than having the simulation run for 3 seconds while capturing a result every 0.1 seconds. This allows the ability to see the development of the system prior to reaching the steady state solution. Changing only one variable at a time also allows us the identification of any new effects as well as helping to troubleshoot should any issues arise.

Ultimately, adding time dependency created new issues and requirements for COMSOL. The first issue encountered was the inability of the mesh to handle time dependency in some of the models. COMSOL uses a mesh to determine specific points at which to calculate a solution, and interpolates all other data between these points. COMSOL allows for specific conditions to be adjusted manually for the mesh, however the most practical and efficient method for our models was to use the preset conditions.

Using the preset options only required a selection of how fine of a mesh was needed for a given model. For these models, a coarse mesh was found to be more than capable of showing the necessary definition. Preset options allow COMSOL to select where to place the points, focusing on placing more points in areas that will be changing more rapidly. COMSOL places the points much more densely near the stenosis, coinciding with the area of interest for this study, as seen in Figure 7.

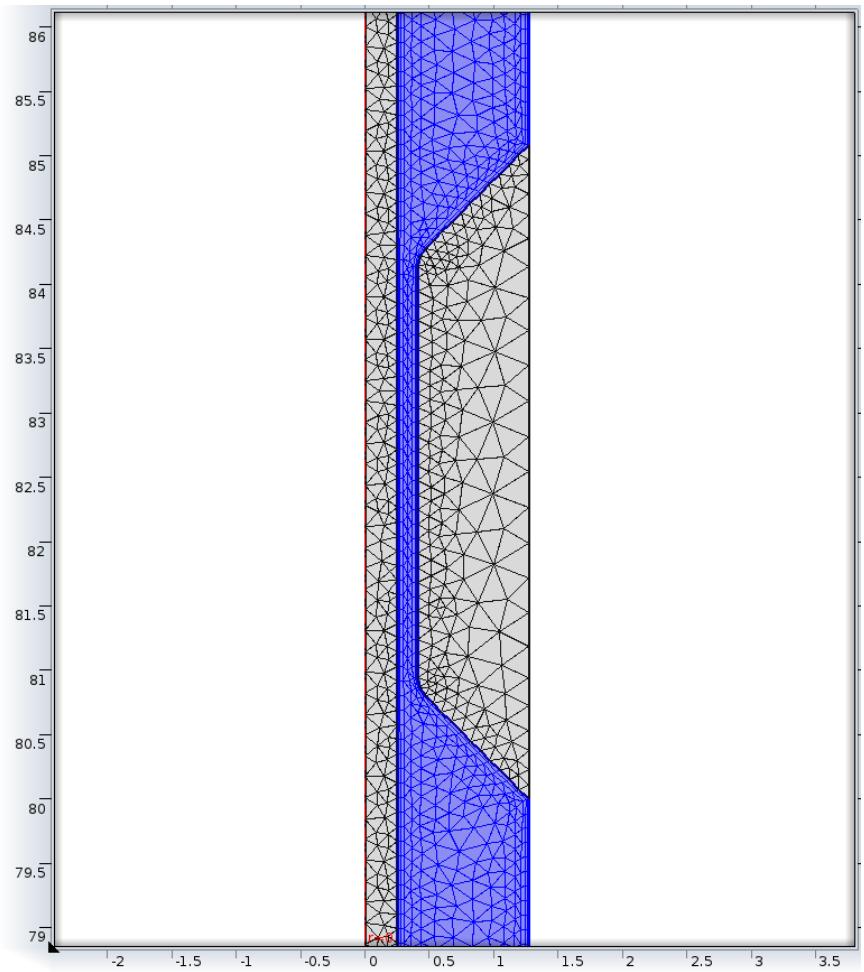

Figure 7. Example of mesh configuration in a 90% stenosis with guidewire model.

Using this method proved very successful for steady state models; however, it created complications when time dependency was introduced. In particular, for the higher grade stenoses (75% and 90%) with guidewire, the model was unable to run using the previous mesh configuration. The use of an "adaptive mesh" feature was required in order to run these time-dependent solutions.

The adaptive mesh feature of COMSOL is only available for time-dependent solutions. The user selects the initial mesh setting that COMSOL uses for the first time step. From that point on, COMSOL creates a new mesh for each given time step, or as specified by the user. While this adds a significant amount of processing time to the computation, it also allows COMSOL to shift the focus of the computations as necessary to capture fluid effects as they develop. This is of particular importance for any fluid

effects that are not permanent or that shift throughout the system. This phenomenon can be seen in Figure 8, where the adaptive mesh shifts the area of focus for computations as an effect moves downstream.

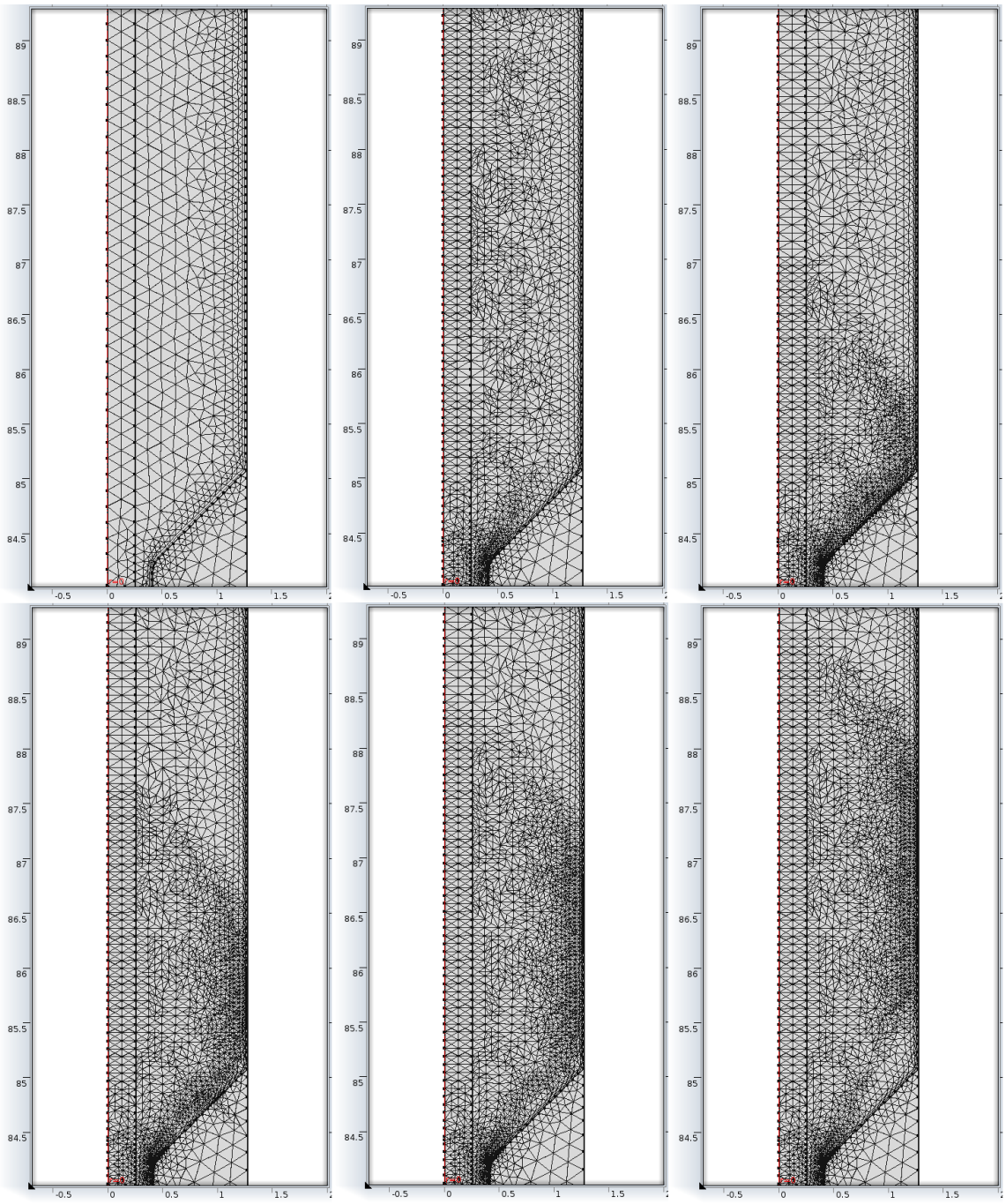

Figure 8. Example of self-adjustments made by adaptive mesh. All units are in centimeters.

B. NEW EFFECTS IN TIME-DEPENDENT MODELS

As expected for the lower stenoses (20, 40 and 60%), the effect downstream was fairly insignificant. For the higher grade stenoses, the effect was very minimal as well with no guidewire. This, too, was expected, as the reduction in area was far less significant than the 75% and 90% with guidewire models.

As a result, the primary concern with this effect was the 75% and 90% models when the guidewire was present. Both of these models showed fairly significant amounts of disruption in the initial downstream flow following the stenosis, although this was far more drastic with the 90% (Figure 9).

For both of these models, however, the phenomenon resulted in initial eddies that were ultimately pushed through the system, explaining why the effect was never seen during the steady state simulations.

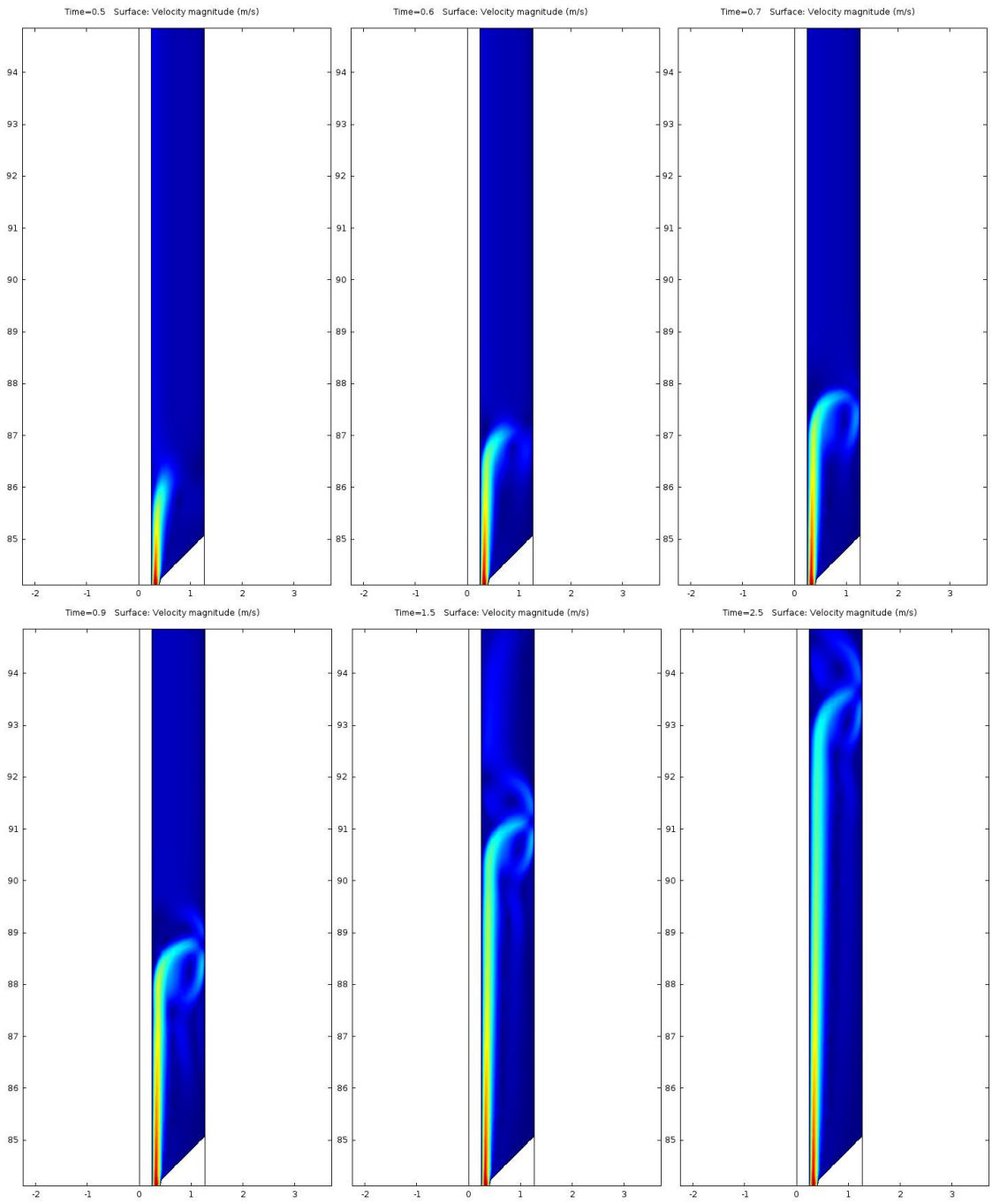

Figure 9. Time lapse of the formation and movement of flow using a steady input, 90% stenosis, and guidewire.

This behavior raised more questions. Due to the steady state nature of the model in previous simulations, the disruption downstream was fairly insignificant. It was present only on the initialization of the flow, ultimately, dissipating in time. The final

desired system, however, requires pulsatile flow, meaning that an effect on an increase of flow could still be relevant to the end result, and the ability to capture this effect is essential in order to understand how the system behaves.

III. COMPUTER SIMULATIONS

A. 20% STENOSIS

1. No Guidewire Case

In order to achieve a 20% area reduction in the cylinder, the stenosis was simulated using a trapezoid with its base along the outer wall with a length of 5.08 cm (two tube diameters). Both ends leading to the inner wall of the stenosis had an angle of 45 degrees to achieve a height of 0.13 cm and an inner length of 4.69 cm when rounding of the corners is taken into consideration. The vertices of the stenosis wall were rounded by means of a fillet geometry function with a radius of 0.2 cm to approximate the machining characteristics of the actual acrylic stenosis used in the experiment. Rounding the corners, as compared to using sharp corners, had no effect in the velocity profiles for any of the stenoses used. However, it did have a large effect in the shear rate magnitudes not only at the vertices of the stenosis but throughout the stenosis length as well. A default physics-controlled mesh was used with a "Fine" element size (Dean 2013).

For the Re300 (Reynolds number 300) 20% stenosis with no guidewire present, an average input velocity of 4.74 cm/s was chosen (compared to an average input velocity of 3.16 cm/s obtained in the Re200 experiment). This velocity is first approximated by setting r = 0 in Eq. (2) to find the average velocity of the fluid from the maximum experimental velocity obtained at the -1.5D position. The average velocity obtained was 4.72 cm/s, but this value is not precise due to the errors in the experimental measurement of the velocity. The average velocity is then adjusted to better match the experimental results. The dynamic viscosity for the experiment was 4.4745 mPa*s, and the fluid density was 1115.5 kg/m^3. A no-slip boundary condition is enforced at all points along the outer wall including the stenosis.

Figure 10 shows the comparison of measured and simulated velocity profiles. In order to plot velocity profiles for all axial locations on the same graph, a 10 cm/s velocity offset was added to each progressive profile in order to place it in the right vertical spot on the graph.

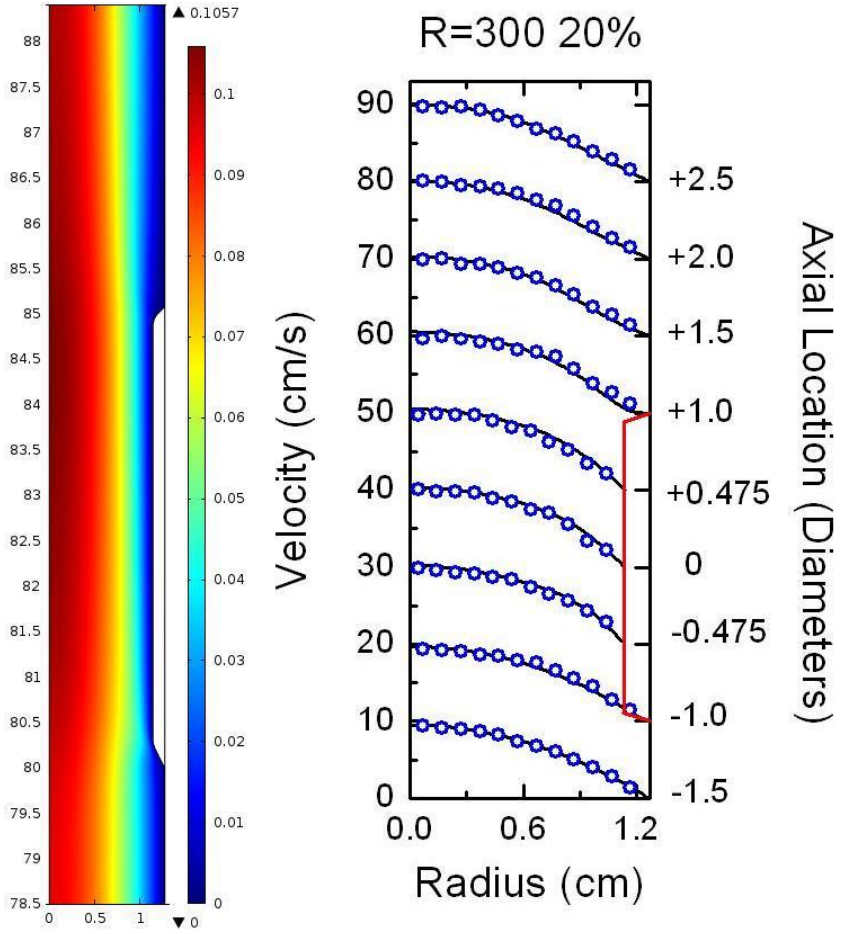

Figure 10. Velocity profile for the 20% stenosis. The computer simulation is displayed on the left in m/s. Velocity profiles at specific axial locations are displayed on the right against experimental data (blue circles) in cm/s. Velocities for each axial location are spaced by 10 cm/s intervals.

The highest velocity measured experimentally was 10.15 cm/s at the 0 (mid-stenosis) axial location, while the simulation yielded a value of 10.39 cm/s for the same location. A good agreement between the measured and simulated velocity profiles can be seen in Figure 10.

2. Guidewire Case

The setup is the same as the no guidewire case, with the exception of the inclusion of the guidewire at the center of the pipe. Average input velocity used was 4.5 cm/s. In this case, Eq. (2) will provide a less accurate approximation to the average inlet flow velocity required, given that the measured flow at the guidewire wall does not go to zero.

The same phenomenon of non-zero velocity at the guidewire wall observed by Dean in the Re200 simulation as appears in the Re300 simulation, albeit at a higher magnitude.

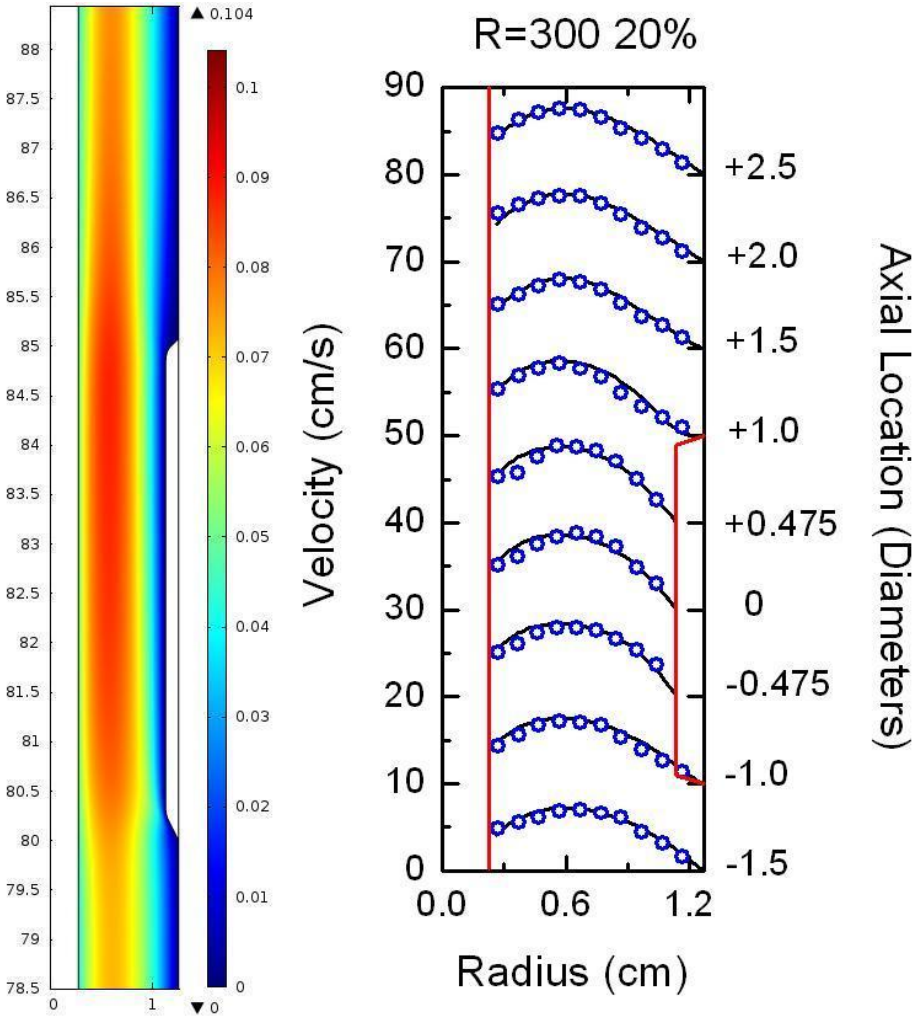

Figure 11. Velocity profile for the 20% stenosis with guidewire present. Computer simulation is displayed on the left is m/s. Velocity profiles in cm/s displayed on the right against experimental data (blue circles).

The experimental results in Figure 11 show that the velocity of the flow at the point closest to the guidewire at the -1.5D location is 1.55 cm/s, at -1.0 the velocity is 1.41cm/s, and inside the stenosis the velocity closest to the guidewire surface goes up to 3.63, 3.01 and 2.6 cm/s for the -.475D, 0.0D, and +.475D locations, respectively. In order to simulate this non-zero velocity phenomena observed at the guidewire surface, a slip-

velocity boundary condition was set along the guidewire wall using a slip length *Ls* of 1.7 mm. The maximum experimental velocity recorded for this stenosis was 8.86 cm/s at the 0.0D axial location, compared with a value of 8.26 cm/s obtained from the simulation at the same axial location. A good agreement between the measured and simulated velocity profiles can be seen in Figure 11.

B. 40% STENOSIS

1. No Guidewire Case

The dynamic viscosity and density of the fluid used for the 40% stenosis simulation were the same values as the 20% stenosis given that the same fluid was used for the experiment. The 40% constriction is achieved by giving the stenosis a height of 0.29 cm. Since the outer length of the stenosis and the angles are fixed to two diameter lengths and 45 degrees respectively, the inner length of the stenosis is 4.21 cm. Fillets of radius 2 cm were used to round the corners of the vertices. Figure 12 displays the measured and simulated velocity profiles.

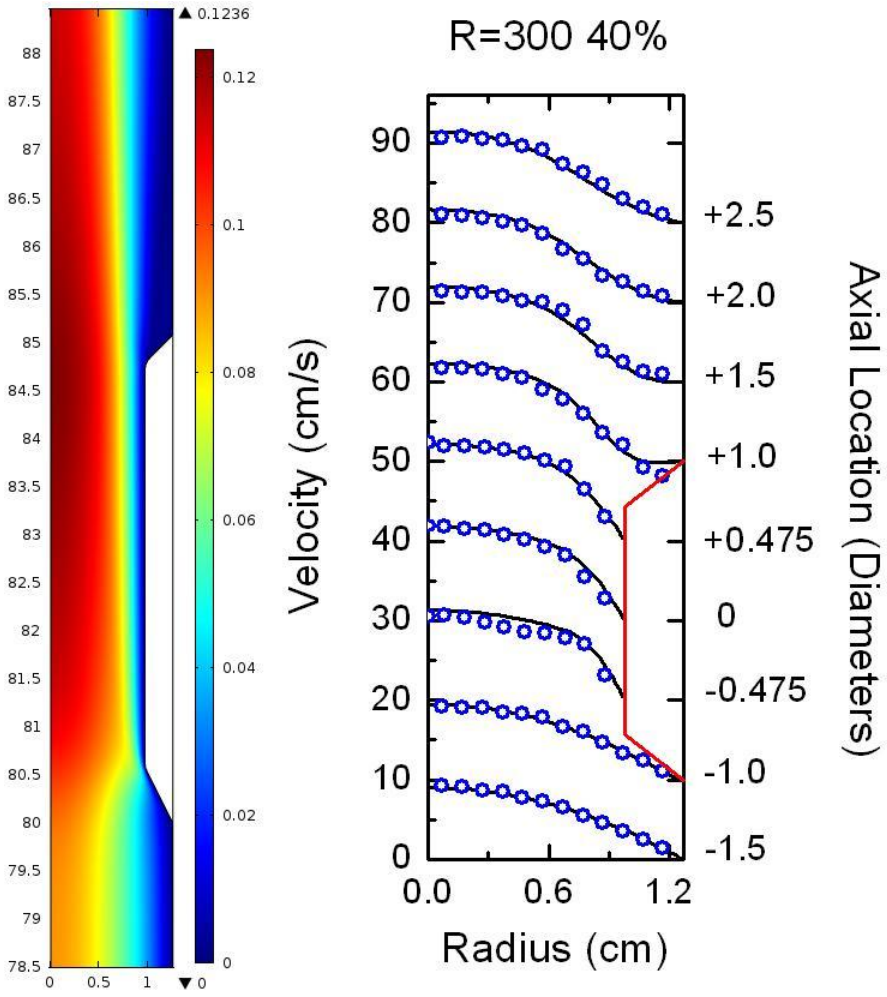

Figure 12. Velocity profile for the 40% stenosis with no guidewire. Velocities for each axial location are spaced by 10 cm/s intervals.

The maximum experimental velocity recorded was 12.32 cm/s at the +.475D axial location compared to a value of 12.23 cm/s obtained from the simulation at the same location. A good agreement between the measured and simulated velocity profiles can be seen in Figure 12.

2. Guidewire Case

The fluid properties were the same as the ones used for the no-guidewire case. A constant moving wall velocity at the guidewire was not able to replicate the experimental results given that a larger velocity was required near the guidewire wall at the stenosis height. However, the slip velocity boundary condition with viscous slip with slip length

of 0.88 mm was able to replicate the experimental results at the guidewire. Figure 13 shows the comparison of measured and simulated velocity profiles. There is still a discrepancy at the -.475D position close to the stenosis wall that is due to the no-slip boundary condition forced at the stenosis wall. The 40% stenosis with guidewire simulation is the smallest stenosis to form a recirculation region past the exit of the stenosis, where a maximum negative velocity of -3.27 cm/s occurs.

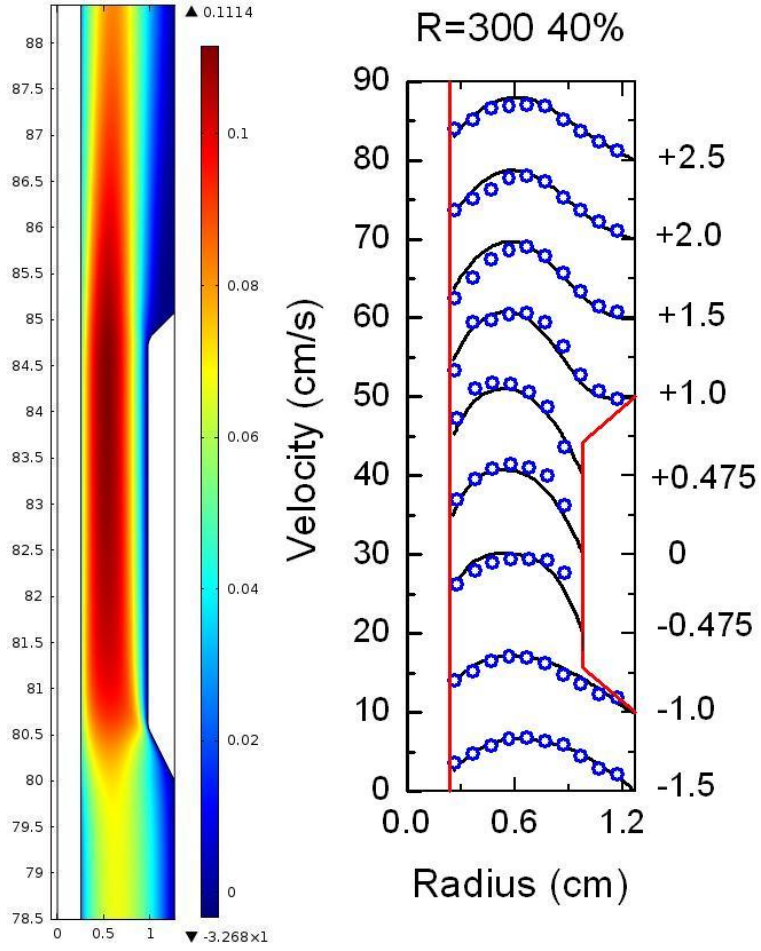

Figure 13. Velocity profile for the 40% stenosis with guidewire. Experimental data show a slip boundary condition at the entrance of the stenosis, while the no-slip boundary condition imposed on the simulation forces the velocity to go to zero.

The 40% stenosis forces the experimental velocity recorded closest to the guidewire wall to increase from 4.03 cm/s at the -1.0D location to 6.25, 6.92, and 7.29

cm/s for the -.475D, 0.0D and +.475D locations, respectively. The slip velocity boundary condition established at the guidewire surface is able to mimic this rise in velocity inside the stenosis, where clearly a constant moving wall velocity would fall short of accomplishing the same result. The maximum experimental velocity observed was 11.72 cm/s at the +.475D location, midway between the stenosis and guidewire walls. The simulation velocity obtained at the same point was 11.07 cm/s.

C. 60% STENOSIS

1. No Guidewire Case

The 60% constriction is achieved with a stenosis height of 0.47 cm, which yielded an inner stenosis wall length of 4.14 cm. The dynamic viscosity for the experiment was 6.2536 mPa*s and fluid density of 1133.2 kg/m^3. A no-slip boundary condition is enforced at all points along the outer wall including the stenosis. Input velocity had a value of 6.1 cm/s. The 60% stenosis is the lowest grade stenosis to yield a negative velocity due to backflow when no guidewire is present. Figure 14 shows the measured and simulated velocity profiles.

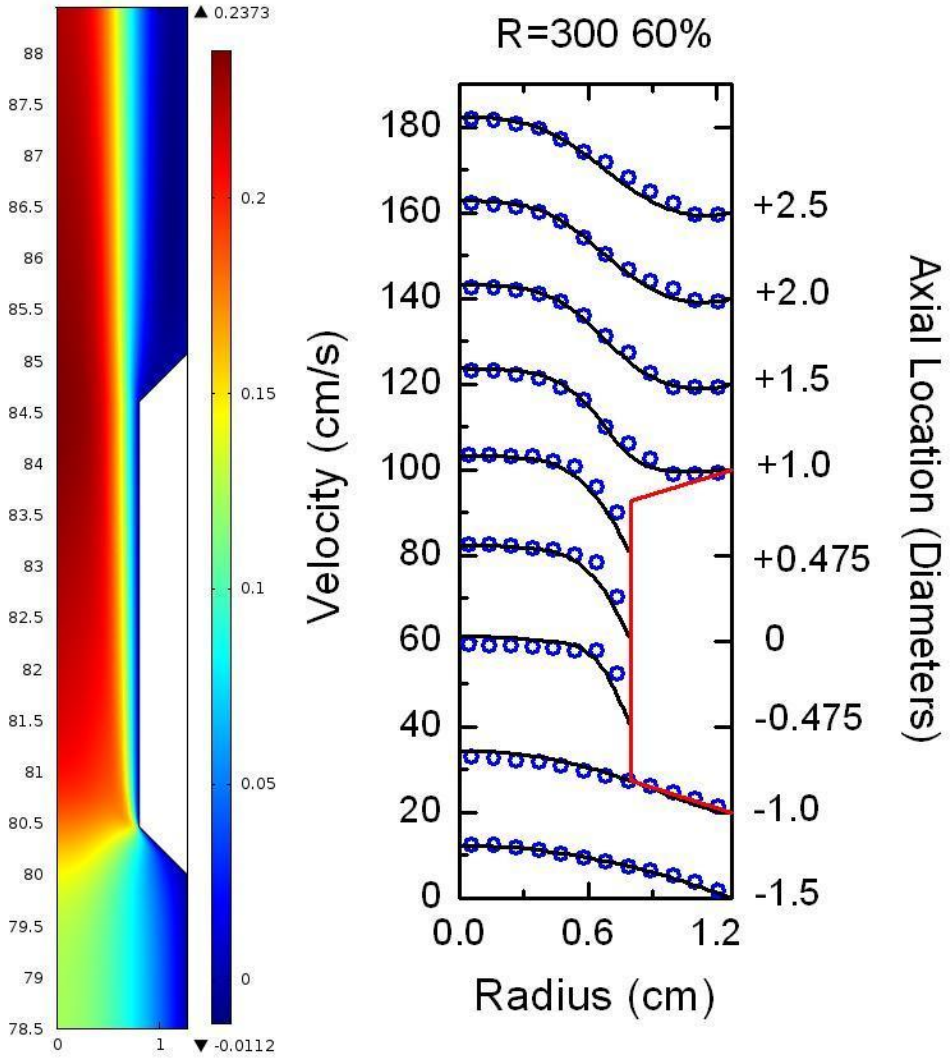

Figure 14. Velocity profile for the 60% stenosis. Experimental values show a non-zero velocity at the surface of the stenosis. Velocities for each axial location are spaced by 20 cm/s intervals.

Backflow occurred past the stenosis and reached a maximum speed of 1.12 cm/s. The highest fluid velocity from the simulation was 23.73 cm/s and occurred centerline between the +.475D and +1.0D locations, coinciding with the location where the stenosis ended. The maximum value obtained from the experiment occurred at the +1.0D location closest to centerline with a value of 23.08 cm/s, versus 23.64 cm/s obtained by the simulation at the same location.

2. Guidewire Case

The same fluid from the no guidewire case was used. The average input velocity was 6.5 cm/s and a viscous slip boundary condition with slip length 1.5 mm was used at the guidewire. An exponentially decaying moving wall boundary condition was attempted in order to replicate the behavior near the stenosis wall at the -.475D position. This exponentially decaying velocity function was successful at replicating the experimental results. However, the experimental data does not include values for the velocity close to the stenosis wall. As a result, many different values for the amplitude and decay constant for the exponentially decaying velocity function could replicate the experimental results. A no-slip boundary condition was decided for all stenoses until a new experiment is performed with better velocity resolution near the stenosis walls.

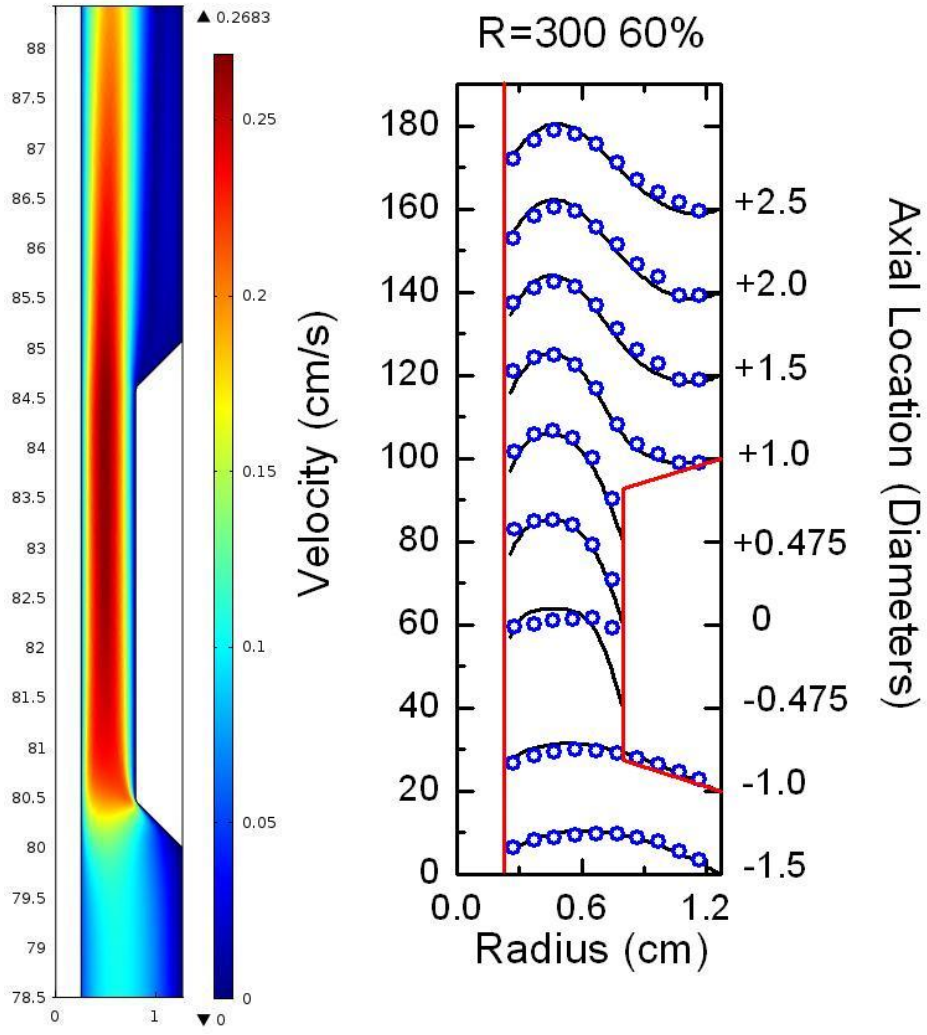

Figure 15. Velocity profile for the 60% stenosis with guidewire.

The addition of the guidewire increased the maximum fluid velocity from 23.73 cm/s to 26.83 cm/s at a location 0.4 cm away from centerline and a position of +0.7D. The highest velocity measured experimentally occurred at the +.475D position with a value of 26.52 cm/s, compared with 26.06 cm/s from the simulation at the same location. The highest velocity from the simulation occurred at the +.7D location with a value of 26.83 cm/s.

D. 75% STENOSIS

1. No Guidewire Case

The 75% stenosis constriction is achieved with a stenosis height of 0.635 cm, which yielded an inner stenosis wall length of 3.81 cm. The dynamic viscosity for the experiment was 11.833 mPa*s and fluid density of 1167 kg/m^3. Input velocity for the simulation had a value of 13.8 cm/s. Due to the small cross-sectional area caused by the presence of a large stenosis the number of measurements inside the stenosis was doubled, as shown in Figure 16. This was done by measuring at a distance of half a millimeter between measurements compared to one millimeter for lower stenoses.

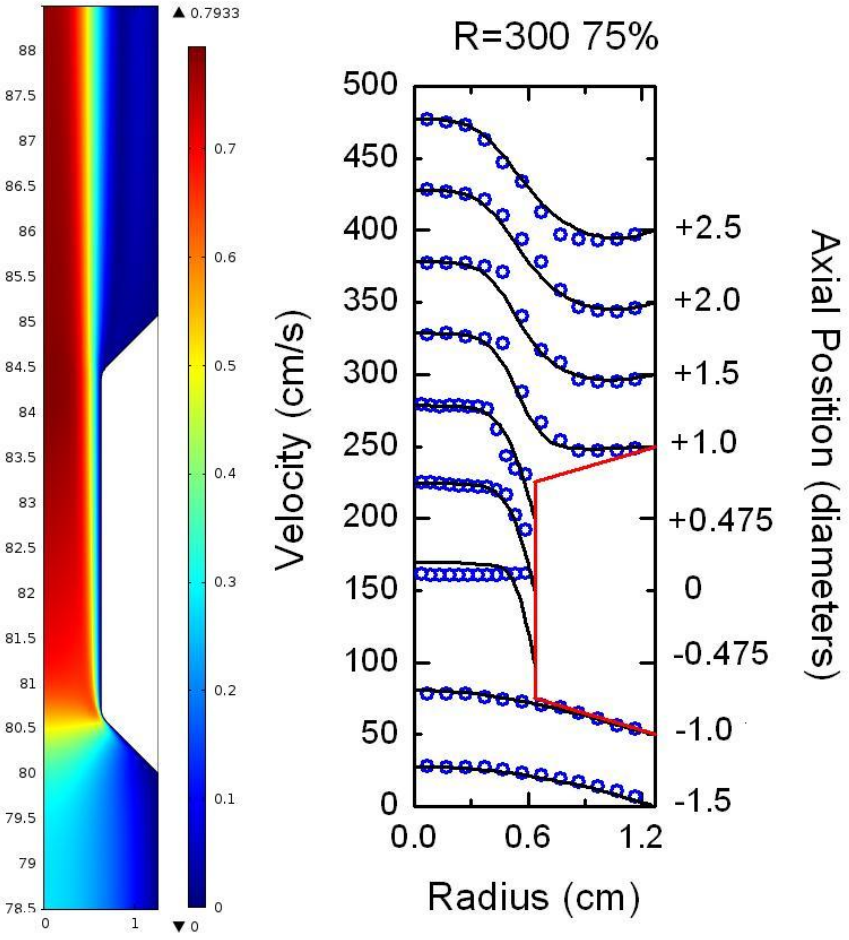

Figure 16. Velocity profile for the 75% stenosis with no guidewire.

The reason the velocity profile throughout the channel is higher in the simulation for the -.475D position is because of the no-slip boundary condition imposed at the stenosis wall, which by conservation of mass forces the flow to have a higher velocity throughout the rest of the channel. The highest simulation velocity had a value of 79 cm/s at the +0.7D diameter position. The maximum experimental velocity of 78.81 cm/s occurred at the +.475D position. The velocity obtained from the simulation for the same point was 78.41 cm/s.

2. Guidewire Case

In contrast to all previous stenosis data, the 75% stenosis experimental data required a normalization factor to account for the fact that three different fluids with different densities and viscosities were used for the experiment. Fluid one had a viscosity of 11.833 mPa*s, a density of 1167 kg/m^3,and was used for the -1.5D measurement. Fluid two had a viscosity of 4.175 mPa*s, density of 1112 kg/m^3 and was used for the -+1.0D measurement. Fluid three had a viscosity of 5.119 mPa*s, a fluid density of 1123 kg/m^3 and was used for the -.475D, 0.0D, +.475D, +1.0D and +2.5D measurements. Previous attempts at matching the simulation to experimental data failed because only fluid three was used for the simulation. It was discovered that although different fluids may be normalized by means of taking the ratio of their viscosities and densities, the slip velocity at the guidewire wall depends non-linearly on the fluid's viscosity. Therefore a different simulation was required for each fluid. The simulation for fluid one used an input velocity of 5.67 cm/s and a viscous slip boundary condition at the guidewire surface with a slip length of 2.5 mm; the simulation for fluid two used an input velocity of 4.58 cm/s and a slip length of 2.5 mm, and the simulation for fluid three used an input velocity of 5.72 cm/s and a slip length of .5 mm. To be able to plot the experimental data for all locations on the same graph, the results for the -1.5D and -1.0D values were normalized to fluid three's values. Figure 17 shows the comparison of measured and simulated velocity profiles.

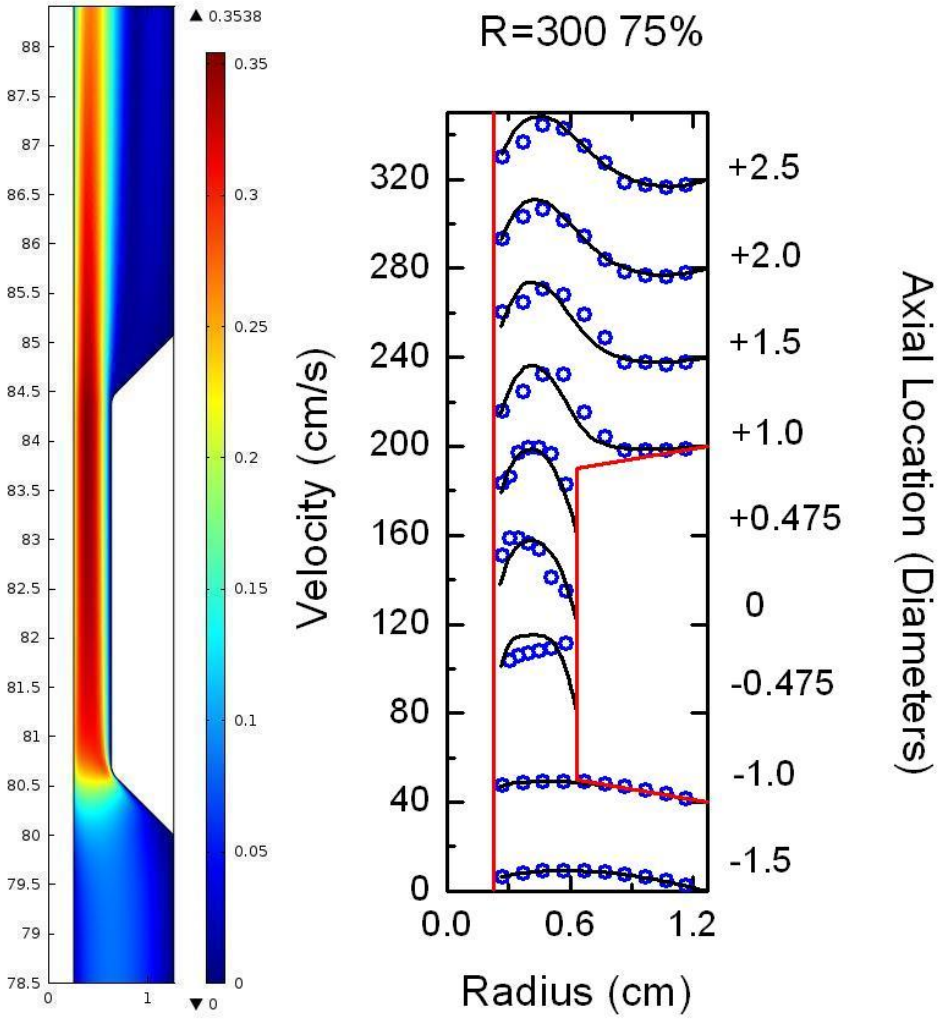

Figure 17. Velocity profile for the 75% stenosis with guidewire.

The highest experimental velocity obtained was 39.43 cm/s at the +.475D location compared with a simulation value of 35.15 cm/s at the same location. The largest discrepancy occurs at the stenosis surface for the -.475D location, and it is due to the no-slip boundary condition imposed on the stenosis surface which forces the velocity to go to zero.

E. 90% STENOSIS

1. No Guidewire Case

The 90% stenosis constriction is achieved with a stenosis height of 0.86 cm, which yielded an inner stenosis wall length of 3.36 cm. The 90% stenosis without guidewire experimental setup required two fluids. Fluid one was used for the -1.5D, -1.0D and -.475D positions, with a viscosity value of 11.833 mPa*s and density of 1167 kg/m^3. Fluid two was used for the 0.0D, +.475D, +1.0D, +1.5D, +2.0D and +2.5D positions with a viscosity of 4.175 mPa*s and density of 1112 kg/m^3. Normalization of experimental values was required as was the case for the 75% stenosis with guidewire. The simulation was run using fluid two's properties. The average input velocity was 4.5 cm/s. Figure 18 shows the measured and simulated velocity profiles.

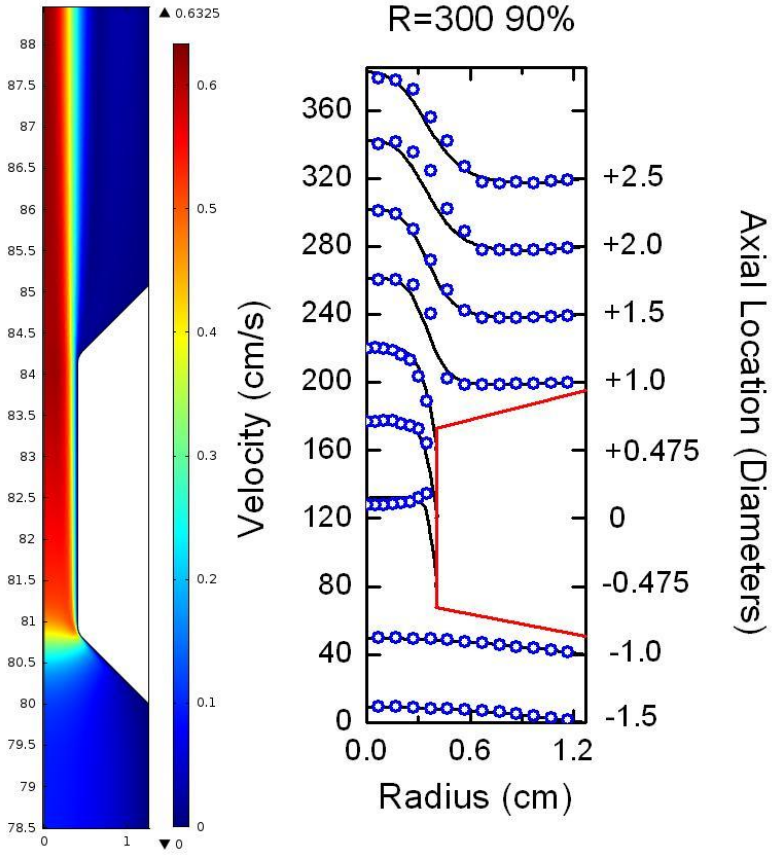

Figure 18. Velocity profile for the 90% stenosis.

For the 90% stenosis without guidewire setup, the maximum velocity did not occur at a location that matched the location of the stenosis. Instead, the maximum experimental velocity occurred at the +1.5D axial location, with a value of 60.49 cm/s, compared with 61.78 cm/s obtained from the simulation at the same location.

2. Guidewire Case

For the 90% stenosis with guidewire, two different fluids were used and normalization was performed to graph the results. Fluid one had a viscosity of 4.4745 mPa*s and density of 1110 kg/m^3. It was used for the experimental measurements at the -1.5D, -1.0D and -.475D positions. Fluid two had a viscosity of 4.175 mPa*s and a density of 1112 kg/m^3. Similar to the 75% stenosis with guidewire case, a simulation had to be run for each fluid to account for the non-linear characteristics of the slip velocity at the guidewire surface. Fluid one used an input velocity of 4.7 cm/s and a slip velocity boundary condition at the guidewire wall with slip length of 0.1 mm and fluid two used an input velocity of 5.2 cm/s with a slip length of 0.3 mm. The outer wall (including the stenosis) had a no-slip boundary condition. From Figure 19 it is clear that the simulation cannot match the experimental results at the guidewire wall.

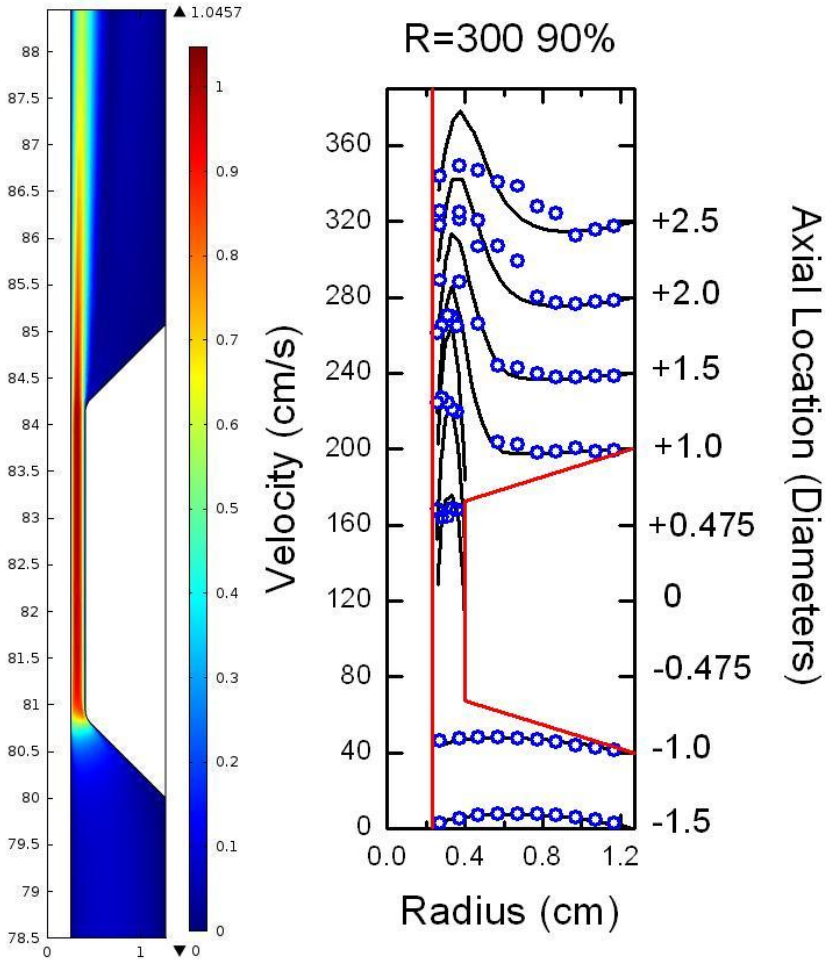

Figure 19. Velocity profile for the 90% stenosis with guidewire.

The velocity of the fluid near the guidewire in the 90% simulation with guidewire is smaller than the experimental results. Contrary to the 75% simulation with guidewire, the 90% simulation is not able to match experimental results properly for the downstream axial locations. This is caused by the no-slip boundary condition which forces the velocity at the stenosis wall to be zero, therefore increasing the flow near the guidewire. By the time the fluid exits the stenosis, the fluid flux is still concentrated in the central regions of the channel, so the magnitude of the velocity has to be higher in the open area of the channel, overshooting the experimental results. The 75% simulation is still able to match experimental results downstream because by the time the fluid passes the +.475D location the experimental fluid velocity near the stenosis wall approaches zero and matches the no-slip boundary condition of the simulation. The same shortcoming was

observed by Dean in the Re200 simulation and again by the authors when performing the simulation for Re400 values. The maximum experimental velocity observed was 104.23 cm/s at the mid-stenosis axial location, compared with a simulation velocity of 101.77 cm/s at the same location.

F. SHEAR RATE

An analysis of shear rate was performed using data from the stenosis simulations for both the guidewire surface (when applicable) and the outer wall surface for all stenoses. Shear rate is important in cardiovascular medicine because it affects atherosclerosis (Giddens, Zarins &Glagov, 1993), thrombosis (Badimon, Chesebro & Badimon, 1992), and restenosis after coronary intervention (Koskinas, Chatzizisis, Antoniadis & Giannoglou, 2012). A distance of 1 micron from the surface was chosen for all the shear rate measurements. Shear rate values were readily obtained from the simulations. COMSOL analyzes the shear stress from the numerical simulations and the fluid's viscosity to obtain the shear rate at the desired position. Unfortunately, the results obtained cannot be compared against the experiment data due to the physical limitations of the measuring device. The LDV was not able to obtain precise measurements close to the surfaces, so meaningful shear rate data cannot be extracted from the experiment. The guidewire surface had a slip velocity boundary condition, with a slip length magnitude that matched the conditions already stated for each simulation.

1. Guidewire Surface

It is clear from Figure 20 that the magnitude of the shear rate at the guidewire surface increases as the stenosis grade increases, not only at the axial location where the stenosis is located (-1D to +1D) but throughout the full length of the guidewire. The maximum shear rate magnitude obtained matched the section of the guidewire at an axial distance coinciding with the upstream vertex of the stenosis. The shear rate at the guidewire for 20% stenosis reached a maximum value of 29.73 s^{-1}, which is a 27% increase from the nominal shear rate value downstream of the stenosis. The 40% stenosis had a maximum shear rate magnitude of 57.28 s^{-1}, which was twice as high as the nominal downstream shear rate value of 27.75 s^{-1}. The 60% stenosis had a maximum

shear rate magnitude value of 113.7s^{-1}. Similarly to the 75 and 90% stenoses there is a gradual decrease in shear rate downstream of the stenosis, but the simulation setup is not long enough to achieve a constant shear rate magnitude. The 75% stenosis simulation yielded a maximum shear rate at the guidewire of 258.85 s^{-1} and the 90% maximum was 3200 s^{-1}. The color scale in Figure 20 was chosen so that any value of shear rate above 200 s^{-1} would show as a single color in order to maximize the contrast of the lower magnitude values so the phenomena downstream of the guidewire would be visible.

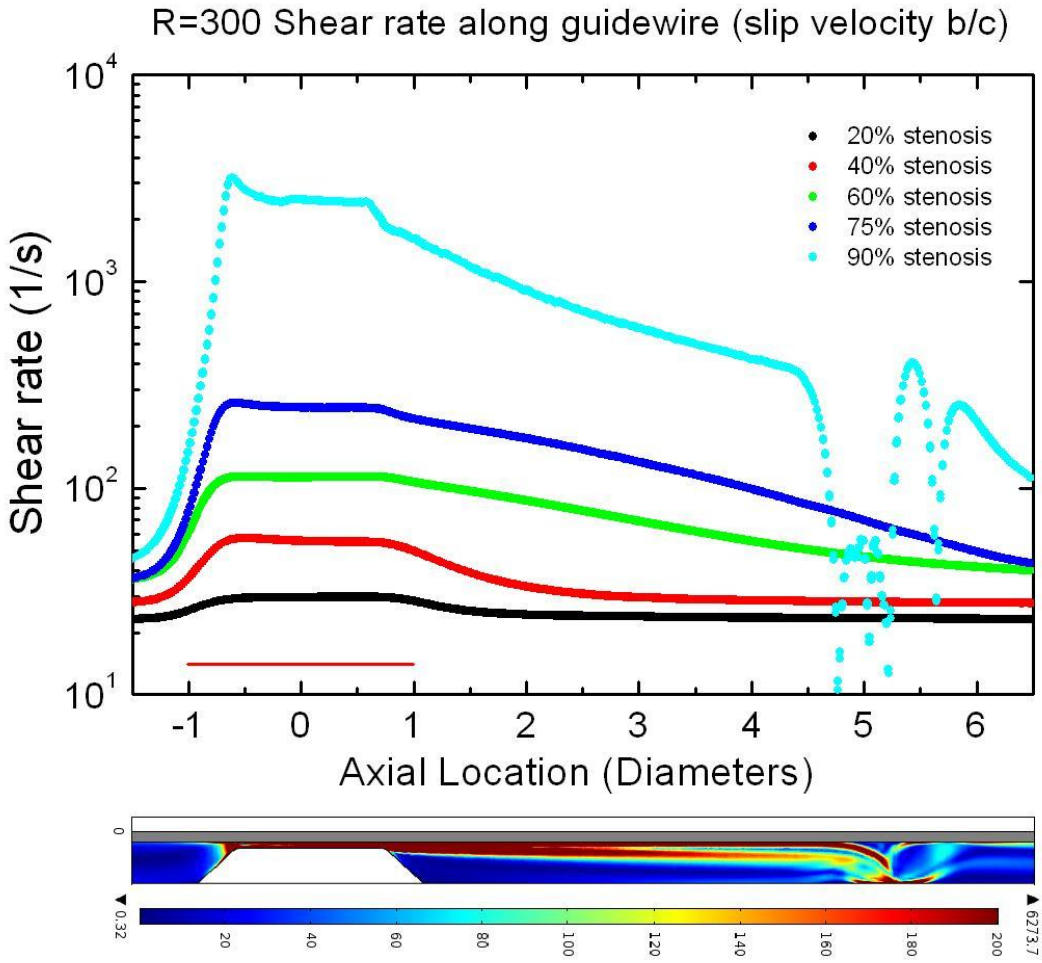

Figure 20. Top: Logarithmic graph of shear rate magnitude 1 micron away from the guidewire units in 1/s. Shown in red is the location of the stenosis along the axial location. Bottom: Shear rate magnitude profile for the 90% stenosis with guidewire.

Figure 20 illustrates that the 90% stenosis simulation exhibits fluctuation of shear rate past the +4D mark downstream of the stenosis. The velocity profile of the fluid shows a recirculation zone that bends the flow towards the outer wall starting at the +4.5D location. As the flow shifts away from the guidewire, the shear rate at the guidewire surface decreases dramatically since the slope of the velocity is less steep due to a recirculation region that emerges at the guidewire at the +5D location, and increases in the space between the guidewire and outer wall as the velocity increases in magnitude and its slope is steeper.

The same shear rate analysis was performed using Dean's moving wall boundary condition at the guidewire for comparison purposes. Even for the smallest of the stenoses the maximum shear rate magnitude varied by as much as 22%. Though either boundary condition was adequate to replicate experimental results of velocity profiles, the moving wall boundary condition provides inadequate results in shear rate. The maximum shear rate recorded at the guidewire was 3200 s^{-1} which occurred for the 90% stenosis case using a slip velocity boundary condition at the guidewire surface, compared to 4661 s^{-1} for the moving wall boundary condition.

2. Outer Wall with No Guidewire

Figure 21 shows the results of measuring the magnitude of the shear rate one micron away from the outer wall for the simulations with no guidewire present. There is a clear pattern inside the stenosis wall of increased shear rate as the size of the stenosis is increased. The maximum value of the shear rate always occurred at the upstream vertex of the stenoses, as shown in Figure 21.

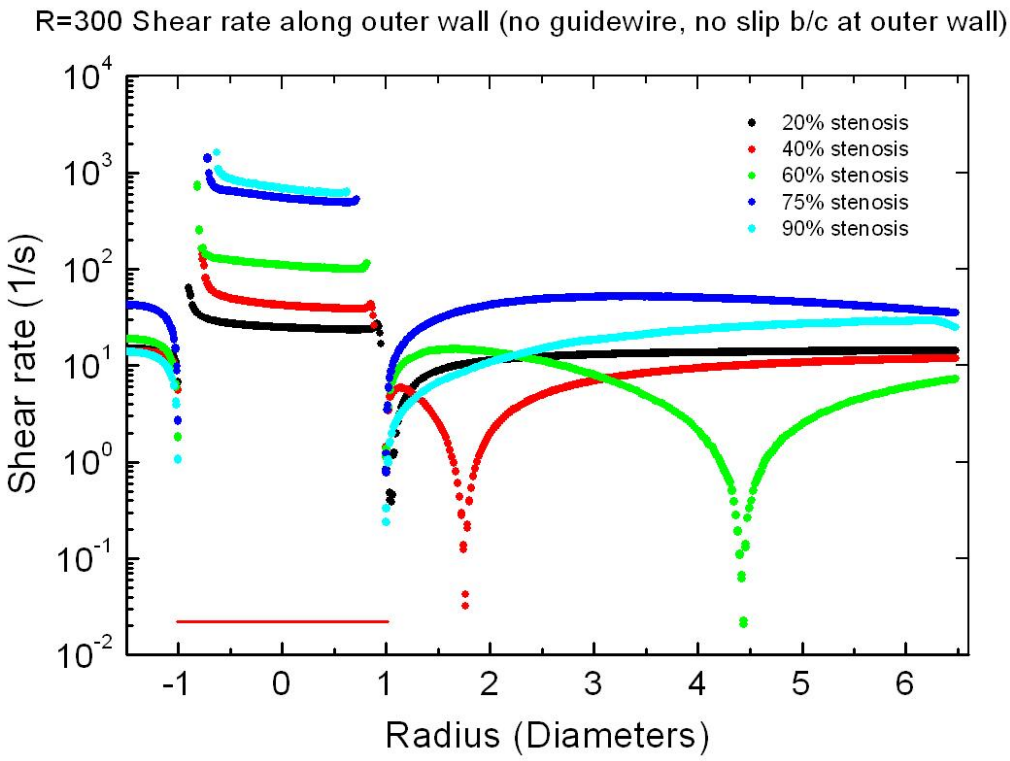

Figure 21. Logarithmic graph of shear rate along the outer wall for simulations with no guidewire present. No slip boundary condition along the length of the outer wall (including stenosis). Units in 1/s.

The maximum shear rates obtained were 63.68, 141.10, 749.45, 1433.04 and 1627.85 s^{-1} for the 20, 40, 60, 75 and 90% stenoses, respectively. Downstream from the stenoses the pattern is more complicated. The 40% stenosis simulation develops a dip in shear rate at the +1.7D location, while the 60% stenosis simulation develops a similar dip at the +4.4D location. The simulation ended at 100 cm to mimic the experimental setup, so the dips in shear rate for the 75% and 90% stenoses are not visible in the figure; however, subsequent simulations proved that the dips do occur further downstream. For the 90% stenosis data, the shear rate just downstream of the stenosis has a smaller magnitude than the rest of the stenoses, indicating a region of near zero flow where the gradient of the velocity is fairly constant near the wall. The maximum shear rate downstream of the stenosis occurred for the 75% stenosis simulation, with a maximum shear rate of 52.25 s^{-1} at the +3.3D location. The maximum downstream value for 60% stenosis was 14.86 s^{-1} at +1.6D, and for the 90% stenosis the maximum shear rate value

obtained was 29.62 s^{-1} at the +6.3D location. Maxima for the 20 and 40% stenoses occurred at points further out from the simulation limit.

3. Outer Wall with Guidewire

Figure 22 shows the results of measuring the magnitude of the shear rate one micron away from the outer wall for the simulations with the guidewire present. The presence of the guidewire increases the shear rate at the stenosis wall for all simulations, as shown in Figure 22.

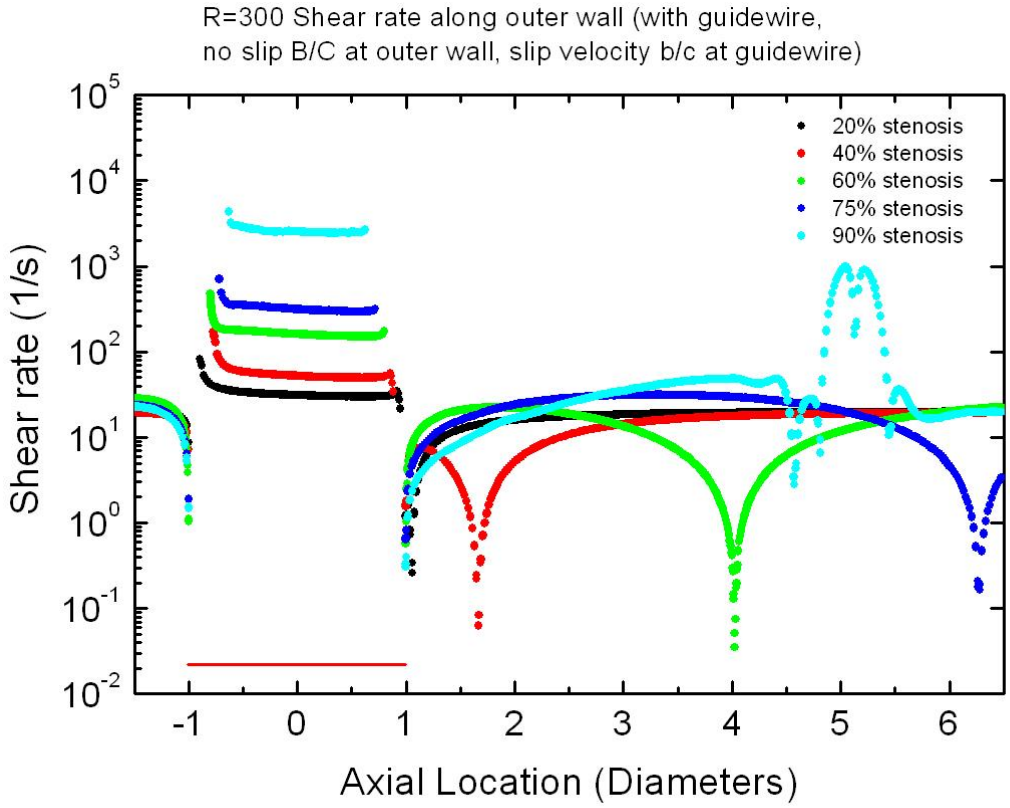

Figure 22. Logarithmic graph of shear rate along the outer wall for simulations with guidewire present. No slip boundary condition along the length of the outer wall (including stenosis). Units in 1/s.

The maximum value of the shear rate obtained was 82.63, 169.80, 479.12, 706.32 and 4315.78 s^{-1} for the 20, 40, 60, 75 and 90% stenoses, respectively. The maximum value always occurred at the upstream vertex of the stenoses. Compared to the previous

study, the presence of the guidewire causes the 75% downstream dip in shear rate to travel upstream to the +6.2D location, compared to +10.4D for the no guidewire case. The 90% stenosis simulation shows a discrepancy that matched the behavior seen at the same axial location in the guidewire as seen in Figure 20. Fluid flow converging from the middle of the channel strikes the outer wall at the +5.2D location, causing areas of high shear rate at the outer wall that reach magnitudes of up to 975.22 s^{-1}.

IV. PULSATILE FLOW

A. SIMULATING A HEARTBEAT

This thesis offers only an initial investigation of pulsatile flow mimicking the human heartbeat. For further development, the velocity profile required to model a human heartbeat must be established. After an extensive literature search, it was determined that a significant amount of future work will be required to determine the various velocity profiles necessary for modeling.

Not only are there variations in the profiles from person to person, but the velocity profile can also change drastically depending on the location within the cardiovascular system being monitored. The first of these two issues will require further research in determining a standard example to use for this system. Ultimately, however, if a sensor is going to be developed for medical use, it must be functional for the full range of profiles that may be encountered.

In order to address the second issue of location within the cardiovascular system, it will be essential to determine velocity profiles in the areas applicable to these medical procedures. While the nature of this problem results in a limited portion of the cardiovascular system, further research will have to be done specifying these locations, determining the individual profiles, and ensuring the sensor is capable of functioning in various environments.

For the purpose of this thesis, we sought only a proof of concept for pulsatile flow to determine what issues are inherent with pulsatile flow being introduced to previous models. To complete this aspect of the model, we required a variable inlet velocity in the general shape of a heartbeat to simulate pulsatile flow.

Using COMSOL, we are able to enter as many or few points as necessary with no requirement for the points to be equidistant in the time scale. COMSOL then uses a piecewise cubic solution to interpolate between the points. The result is the function seen in Figure 23, named beat in the models. This function was used only as a method to scale previous inputs and does not represent the actual inlet velocity in meters per second.

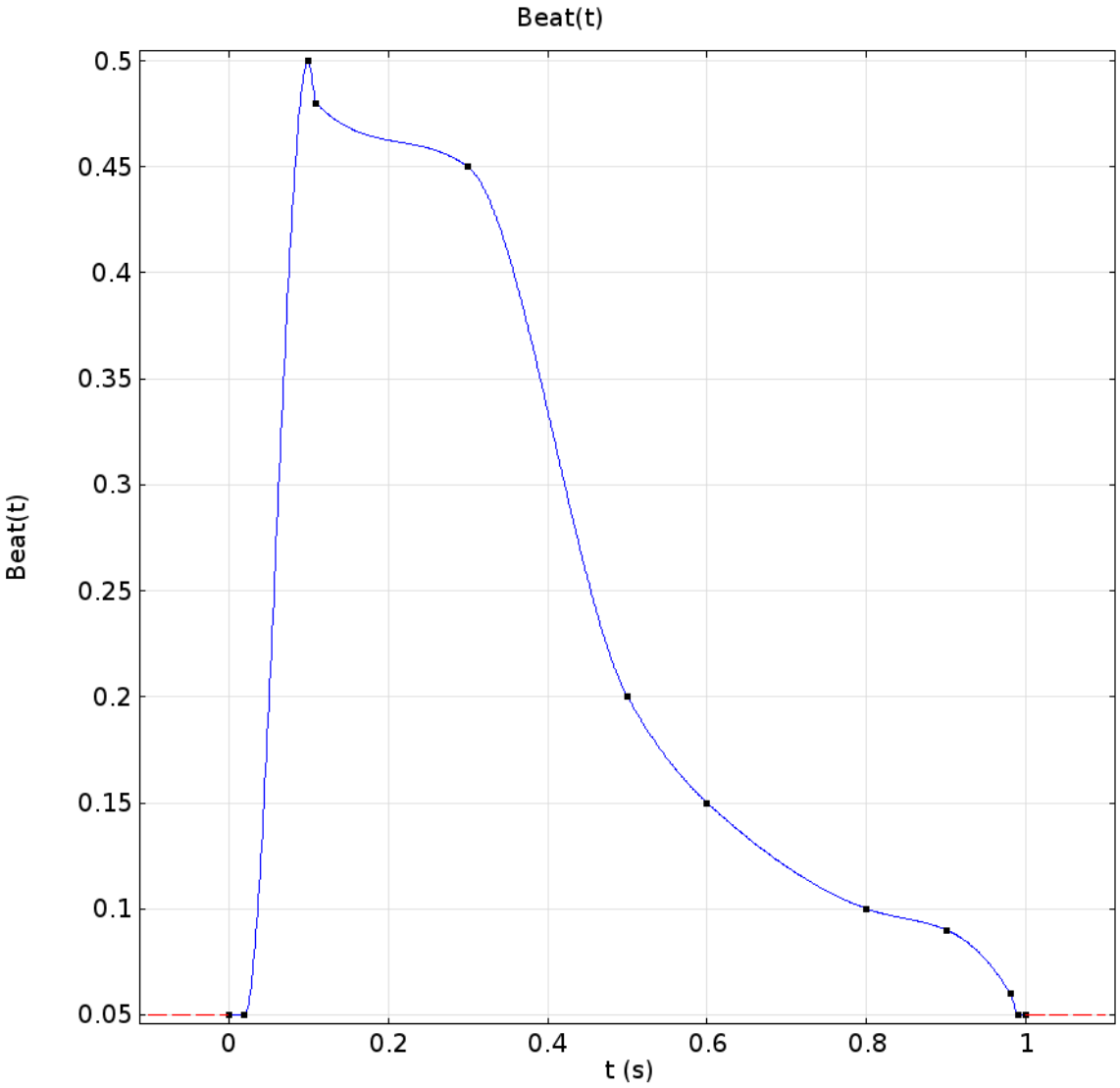

Figure 23. Unitless function applied to pulsatile flow to mimic a heartbeat. Time is in seconds.

Pulsatile flow also requires the use of COMSOL's mod function. This allows for a function (such as the beat function) to be repeated, for the purposes of a these simulations it was repeated once every second. This is critical in order to establish how the system will function in a realistic situation over extended periods of time. By repeating the pulse we are able to determine the effects of a continuous system.

B. RESULTS

As was expected, following the original time-dependent simulations the constriction caused by the higher stenoses when the guidewire was present did result in eddies forming, as seen in Figure 24. These eddies virtually dissipated between pulses and did not continue to flow downstream, but they are significant in the area immediately following the stenosis.

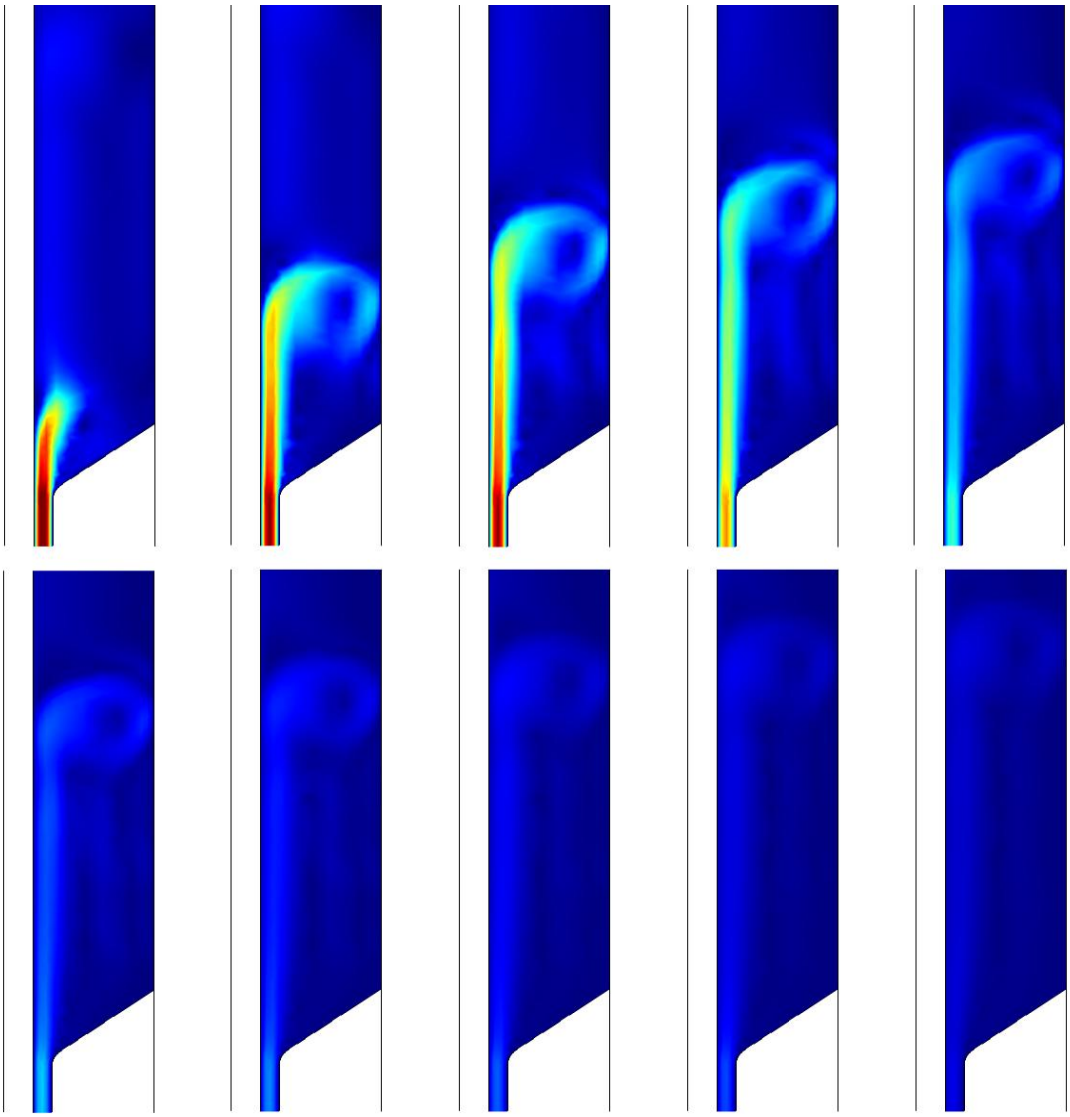

Figure 24. Time lapse of downstream effect in a 90% stenosis model with guidewire using pulsatile flow. Each image represents a 0.1 s time step during a pulse.

It was found that the presence of the guidewire played an even larger role in the formation of these eddies than the size of the stenosis. This is because of the effect it plays in changing the opening area of the tubing. While the reduction in stenosis has a greater effect on the overall area, the guidewire separates the remaining area into two parts, forcing a more drastic affect.

The result is that without a guidewire, even the 90% stenosis shows virtually no effect downstream as seen in Figure 25. Further simulations will have to be completed with a more accurate model of a heartbeat, but these results show that it is likely that a higher level stenosis may have this effect only when the guidewire is inserted. Without the guidewire implanted (as will be the normal case), the effect is most likely going to be negligible.

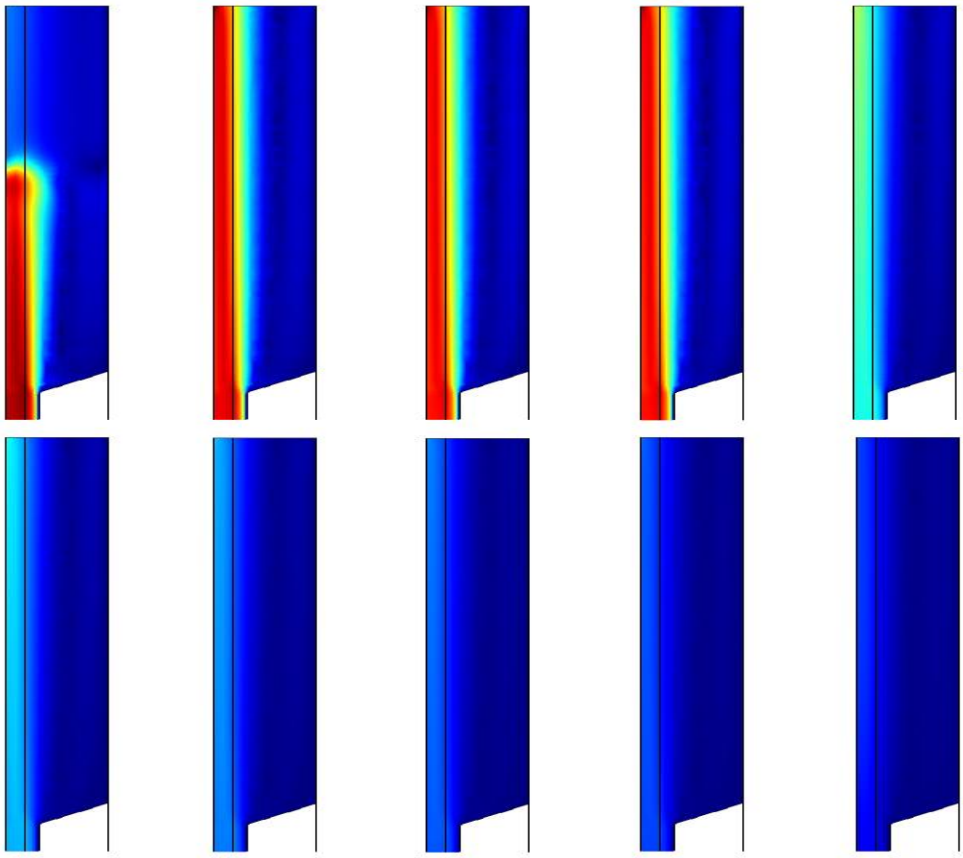

Figure 25. Time lapse of downstream flow in a 90% stenosis model without guidewire using pulsatile flow. Each step requires 0.1 second time step in a pulse.

V. CONCLUSIONS AND FUTURE WORK

Higher processing power and an increase in the number of iterations required by the software solver enabled COMSOL to achieve a steady state solution for all three Reynolds numbers (200, 300 and 400). A non-zero velocity at the guidewire wall caused by a partial slip condition was verified in the experimental results for all Reynolds numbers. The use of a "slip velocity" boundary condition was proven to be successful at simulating experimental results at the guidewire surface for all stenosis grade conditions without the need for the artificial "moving wall" boundary condition used in previous studies, which required arbitrary velocity magnitudes at different points along the guidewire to match experimental results.

The shear rate study at the boundaries provided insights into the shear stresses encountered by the guidewire and outer walls and how their magnitude changes as a function of level of constriction. By running simulations with both moving-wall and slip-velocity boundary conditions at the guidewire wall, it was possible to see the difference in shear rate magnitude encountered when using each boundary condition. Possible causes for the non-zero fluid velocity at the guidewire include the formation of a boundary layer due to the non-hydrophobic paint used for the guidewire or a partial slip condition that occurs due to the irregularities in the guidewire surface. A new experiment with better instrumentation is required to obtain data closer to the boundaries to be able to finally discern the cause of the non-zero velocity at the guidewire wall and at the entrance of the stenosis.

COMSOL proved itself to be capable for both a time dependent study of the model as well as for the application of pulsatile flow. Under some circumstances an adaptive mesh, which significantly increased processing time, was necessary in order to obtain accurate results.

In order to continue developing the model for cardiovascular purposes an accurate range of heart beat models will need to be developed in order to ensure that the system is applicable to modeling a wide range of patients. This will require extensive research into

both the ranges of velocity profiles that vary between patients as well as determining the varieties of profiles based on the location of the stent within the body. Additionally, work will be required to study non-Newtonian fluids in COMSOL in order to more accurately model blood flow.

Once a heartbeat has been sufficiently modeled a fluid structure interaction will need to be developed to begin modeling the desired sensor. COMSOL has this capability although it has not currently been tested for the models used in this thesis. COMSOL also has the capability to model piezoelectric materials that can be used to create a sensor that generates its own power.

LIST OF REFERENCES

Badimon, L., Chesebro, J.H. & Badimon, J.J. (1992) Thrombus formation on ruptured atherosclerotic plaques and rethrombosis on evolving thrombi. *Circulation*. 86(6 Suppl): III74–85.

Cengel, Y.A. & Cimbala J.M. (2006). *Fluid Mechanics Fundamentals and Applications* (3rd ed.). New York: McGraw-Hill.

COMSOL multiphysics. (2013). Theory for the single-phase flow interfaces. Retrieved from http://www.chemeng.lth.se/ketn10/Arkiv/COMSOLdoc4-SinglePhaseFlow_interfaces.pdf

Dean, W.T. (2013). A computer simulation model of fluid flow through a channel with constriction. (Master's thesis). Retrieved from http://calhoun.nps.edu/public/bitstream/handle/10945/34654/13Jun_Dean_William.pdf?sequence=1

Denardo, S., Talbot L., Hargrave, V., Fitzgerald, P., Selfridge, A. & Yock, P. (1994). Analysis of pulsed wave Doppler ultrasound spectra obtained from a model intracoronary catheter, *IEEE Transactions on Biomedical Engineering, 41*(7), 635–648.

Giddens, D.P., Zarins, C.K., & Glagov, S. (1993). The role of fluid mechanics in the localization and detection of atherosclerosis. *Journal of Biomechanical Engineering, 115*(4B):588–594.

Koskinas, K.C., Chatzizisis, Y.S., Antoniadis, A.P. & Giannoglou, G.D. (2012). Role of endothelial shear stress in stent restenosis and thrombosis: pathophysiologic mechanisms and implications for clinical translation. *Journal of the American College of Cardiology*. *59*(15): 1337–1349.

Leimgruber, P., Roubin, G., Hollman, J., Cotsonis, G., Meier, B., Douglas, J., King, S., Gruentzig, A. (1986). Restenosis after successful coronary angioplasty in patients with single vessel disease, *Circulation, 73:*710–717.

THIS PAGE INTENTIONALLY LEFT BLANK

INITIAL DISTRIBUTION LIST

1. Defense Technical Information Center
   Ft. Belvoir, Virginia

2. Dudley Knox Library
   Naval Postgraduate School
   Monterey, California